ORIGINAL PAPER

IoT-integrated smart energy management system with enhanced ANN controller for small-scale microgrid

Alex Mariyaraj[1] · Suresh Padmanabhan Thankappan[2]

Abstract

This research paper focuses on an intelligent energy management system (EMS) designed and deployed for small-scale microgrid systems. Due to the scarcity of fossil fuels and the occurrence of economic crises, this system is the predominant solution for remote communities. Such systems tend to employ renewable energy sources, particularly in hybrid models, to minimize fuel costs and promote environmental sustainability. However, in small-scale microgrids, a significant challenge lies in maximizing power utilization amidst rapid variations in ecological conditions in renewable energy resources, ensuring energy balance during peak demand, and preventing wastage during low demand condition. To address these issues, this research focuses on two main areas. Firstly, the implementation of the GWO-tuned feed-forward neural network MPPT algorithm in both solar and wind energy conversion systems. This control algorithm demonstrates superior performance compared to existing controllers by efficiently tracking the maximum power point (MPP) value and rapidly utilizing the available power. Secondly, IoT-based energy monitoring system is implemented in small-scale microgrid systems to track the real time of data from sources like wind, solar, and batteries. Furthermore, intelligent rule-based strategies are employed to enhance the control function of EMS and ensure stability within the microgrid. This system effectively manages microgrid demand and prevents power wastage. In this specific EMS setup, the battery storage unit is a key component, but challenges arise when there are sudden load and power generation fluctuations, leading to disruptions in control mechanisms. To address this, a GWO-tuned ANN controller is integrated into the voltage control loop of the battery controller unit, effectively correcting DC bus voltage fluctuations and maintaining stability. The entire work has been designed, and system performances are analyzed in the MATLAB Simulink environment and compared with existing work. The simulation results have been validated by means of experimental setup.

1 Introduction

The rapid expansion of industries in modern civilization and excessive use of non-conventional energy sources lead to the energy crisis that suspiciously affects rural communities and also impacts the environment [1, 2]. So, the developing countries are deciding to generate the power through renewable energy sources, in addition to creating the new distribution system for eco-friendly, minimize the operating cost, reduce the power loss, supply continuous power in rural areas and reduce the tariff to consumers [3–5]. The above-mentioned constraints are suitable for microgrid (MG) systems. It consists of renewable energy sources like PV and wind with energy storage systems connected on conventional grid [6–11] as illustrated in Fig. 1.

The majority of benefits are available in microgrid even though some of the technical issues present. The maximum energy utilization in hybrid RES is very difficult because the energy sources are intermittent in nature and the second issue is power balance between sources and sudden raising consumers load [9], due to improper scheduling of the load for non-availability of hybrid energy resource. Furthermore, ineffective control mechanism for battery management system causes cycle aging, temperature sensitivity and an

✉ Alex Mariyaraj
    er.alex03@gmail.com

1   Department of EEE, A.V.C. College of Engineering,
    Mayiladuthurai, Tamil Nadu, India

2   Department of EEE, E.G.S Pillay Engineering College,
    Nagapattinam, Tamil Nadu, India

Fig. 1 Diagram of general microgrid system
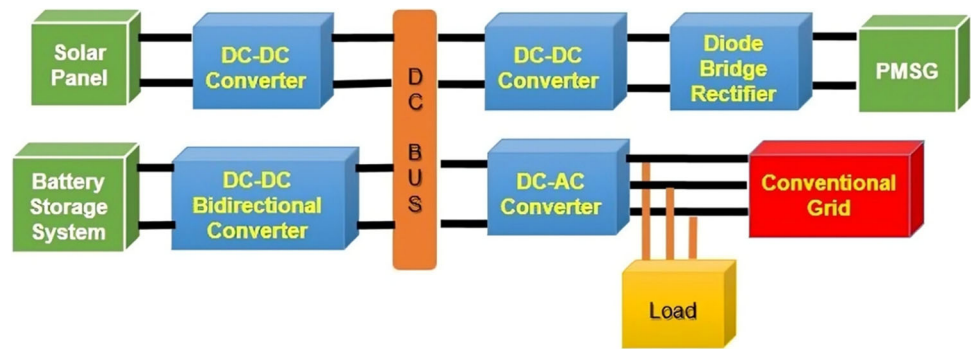
imbalance in the state of charge (SOC), resulting in an unstable DC bus voltage [12–15]. To tackle the mentioned concerns, a proposed intelligent energy management system aims to enhance the performance of small-scale microgrid systems. The energy management primary work is to optimize the use of energy from hybrid resources and minimize energy wastage. [16], second with the absence of hybrid source the battery energy storage system effectively works to maintain power balance to make system reliable, third an islanded mode hybrid power generation-based proper load scheduling action is taken to regulate the voltage and frequency in standard level, and finally, the entire work is smartly monitoring and coordinally controlling the microgrid system to make it reliable, stable and economic [17–22]. In a small-scale microgrid system, a hybrid power source is required to ensure sustainability. Such sources necessitate an efficient controller for optimal utilization of power. In off-grid mode, it is essential to maintain a balance in energy supply by utilizing battery backup with the assistance of advanced controllers for charging and discharging during rapid variations in load and input power. Furthermore, real-time monitoring and a smart management system are crucial for ensuring the reliability and stability of the system. From the above discussion work, the control measures are found based on the literature review step by step.

In the domain of hybrid energy systems, the primary emphasis of researchers is on enhancing energy efficiency and reducing greenhouse gas emissions, specifically in on-grid, off-grid and grid integration scenarios [23–27]. Some scholars delve into the analysis of modeling and sizing hybrid systems [28–30]. One group of authors implemented a hybrid system to provide battery backup for ensuring power reliability to end-users [31, 32]. Furthermore, authors [33] offer a detailed review of the design, modeling and optimization techniques related to hybrid systems. Recent articles indicate that hybrid systems are well-matched for microgrid applications due to their improved power supply reliability, efficient utilization of diverse resources, energy self-sufficiency, and reduced environmental impact. However, certain limitations are also noted, including dependency on weather conditions,

technical challenges such as grid integration and maintaining voltage and frequency regulation in off-grid conditions, as well as the increased complexity in design, control topologies, and maintenance when more renewable energy sources are installed. Based on the aforementioned observation, I deduce that effective control techniques are imperative in microgrid hybrid solar–wind systems with battery integration. Furthermore, a detailed examination of the solar energy conversion system, wind conversion system, and battery storage system control algorithms will be conducted sequentially.

Practically, solar and wind energy conversion efficiency is low such as 17–21% and 20–40%, respectively. The observation must be made that the level of effectiveness in converting energy is of moderate quality, so to enhance the efficiency of converting renewable energy, it is crucial to employ a proficient control algorithm. The solar energy conversion system employs traditional maximum power point tracking (MPPT) algorithms such as hill climbing (HC) [34], incremental conductance (IC) [36, 37], modified incremental conductance method (MICM)[38, 39], perturb and observe (P&O) [40] and finally improved perturb and observe method (IPSO) [41, 42] within its controller and it facilitates the effective tracing of the maximum power point, leading to an overall improvement in system performance. These controlled algorithms are simple, robustness and effectively track MPP in constant ecological condition, but rapid variation of these controller tracking abilities is very less and produced the oscillated reference signal. To overcome this issue, the soft computing-based MPPT methods are developed in past few years like particle swarm optimization (PSO) [43–45], genetic algorithms (GA) [46], grey wolf optimization [47], artificial bee colony (ABC) [48], cuckoo search (CS) [49], ant colony optimization (ACO) [50], cat swarm optimization (CSO) [51], Jaya algorithm (JA) [52], firefly algorithm (FA) [53], bacterial foraging optimization (BFO) [54], flower pollination algorithm (FPA) [55] and gravitational search algorithm (GSA) [56]. These methods have high MPP tracking efficiency, less steady-state oscillation and high conversion ratio, and each algorithm has unique characteristics and used

only particular application. But these soft computing techniques have some certain drawbacks, the GA, PSO, ABC and other metaheuristic optimization algorithms are suffered from computationally expensive, required initial parameter tuning, convergence speed and lack of robustness. Let's now explore intelligent algorithms that are based on human characteristics, like fuzzy logic, and artificial neural networks (ANN). Then the fuzzy logic algorithms struggled to adapt to dynamic and rapid variation in environmental condition and large-scale system to design a fuzzy rules and membership function is very difficult [57–61]. Finally, artificial neural network (ANN) control method is an ability to capture the nonlinear correlation among input and output variables of PV system. So it tracks the accurate MPP and adapts for various ecological conditions in PV system without the need for manual recalibration [62–66]. However, such algorithms have some drawbacks, such as: i) they require ample and meaningful training data to accurately understand the association between input variables (temperature and irradiation) as well as the productivity variable (PV maximum power point voltage (V_{mpp})), ii) ANN parameter tuning (number of hidden layer, weight), and iii) overfitting, which means inaccurate training data or missing data to produce the poor performance in dynamic condition.

Based on my examination of control algorithms for converting solar energy, they can be categorized into three main groups: 1. traditional approaches (like P&O, ICM and HC), 2. soft computing methods (such as PSO, GA, GWO, ACO, ABC, FA and others) and 3. intelligent algorithms inspired by human behavior (like fuzzy and ANN). While these algorithms are appropriate for specific purposes, the rapid fluctuations in environmental data and system requirements may result in limitations, as discussed in the aforementioned literature. The concise literature review can be condensed into Table 1 according to its effectiveness.

In the realm of wind energy conversion systems (WECSs), there exists a captivating pursuit to enhance the power capabilities of the wind turbine. This quest involves the intricate task of tracing and operating at the pinnacle of the turbines power curve, otherwise known as the maximum power point (MPP). In this review section, a detailed overview of the established method of wind energy conversion system (WECS) is introduced. The pitch angle control method [67], tip speed ratio control method [68, 69] and optimal torque control [70] are utilized to enhance the mechanical output power from the wind turbine, known as the indirect control method. On the other hand, methods such as P&O [71] and ICM [72] are employed to directly maximize the obtained output power in the wind turbine, referred to as direct power control. Additionally, as previously mentioned, soft computing techniques such as genetic algorithm (GA) [73], particle swarm optimization (PSO) [74], cuckoo search (CC) [75] and grey wolf optimization (GWO) [76]

are employed to optimize the generator power. Furthermore, human intelligent-based algorithms such as fuzzy logic [77] and artificial neural network (ANN) [78] exhibit more advanced capabilities compared to the aforementioned methods for maximizing power utilization from WECS. Various MPPT methods have been reviewed and scrutinized for their advantages and disadvantages, and improvements are recommended in Table 2.

In rapid variation load (or) renewable energy resources absence, the energy storage system is needed for microgrid system especially for islanded mode. But it is a challenging task to transfer power in a storage device to load and RES to storage device; the bidirectional power flow operation is done in an effective controller. In recent years, many controllers are created for the battery energy storage system (BESS) such as PI [79], PID [80], single phase shift [81], extended phase shift [82], dual phase shift [83], fuzzy logic [84, 85], sliding mode controller [86] and model predictive controller [87]. While these controllers are effective in situations where input parameters experience minor fluctuations, they are not suitable for rapid variations. The existing controller details are mentioned in Table 3. In addition, certain important actions are required in BESS. This includes consistently monitoring the battery's state of charge, current and voltage to improve its lifespan and decrease stress on the battery and finally regulating battery charging and holding the discharging within the boundary condition.

Within a microgrid energy management system, the primary function is to conduct various tasks such as monitoring, analyzing and predicting power generation from renewable energy resources, load consumption, energy market prices, ancillary market prices and weather conditions. These tasks assist the EMS in optimizing the operation of the microgrid, while ensuring technical constraints like energy balance, operational and maintenance costs of the energy storage system, demand response, operational and maintenance costs of traditional generators, reliability, greenhouse gas emission costs, and more are met. Many researchers have explored EMS strategies using different methods to achieve the best and most effective operation of the microgrid. In my detailed examination of microgrid energy management system (EMS), various researchers are employing the following methodologies: linear and nonlinear programming methods [79, 80], dynamic programming [81, 82], rule-based methods [83, 84], metaheuristic approaches (such as matrix real coded genetic algorithm [94], particle swarm optimization [95], slime mold algorithm [96, 97], cockroach swarm algorithm [98], gravitational search algorithm [99]), artificial intelligent methods (including fuzzy logic [114] and neural networks [115]) and model predictive control [116]. The aforementioned methodologies enable researchers to efficiently optimize their individual work objectives. The

Table 1 SECS MPPT Comparison

MPPT method	Dynamic response	Steady state oscillation	Control accuracy	Tracing speed	Overall efficiency	Sensed parameters	Stability
HC [34]	Poor	Large	Low	Slow	Medium	V & I	Poor
P&O [40]	Poor	Large	Low	Slow	Medium	V & I	Poor
IP&O [41, 42]	Moderate	Large	Accurate	Slow	Medium	V & I	Moderate
INC [36, 37]	Moderate	Large	Accurate	Slow	Medium	V & I	Moderate
MINC [38, 39]	Moderate	Medium	Accurate	Moderate	Medium	V, I,	Moderate
PSO [43–45]	High	Medium	Accurate	Fast	Moderate	Varies	Moderate
GA [46]	High	Medium	Accurate	Fast	Moderate	Varies	High
GWO [47]	High	Zero	Accurate	Fast	High	Varies	High
ABC [48]	High	Small	Accurate	Fast	High	Varies	High
CS [49]	High	Zero	Accurate	Fast	High	Varies	High
ACO [50]	High	Small	Accurate	Fast	High	Varies	High
CSO [51]	High	Zero	Accurate	Fast	High	Varies	High
JA [52]	High	Zero	Accurate	Fast	High	Varies	High
FA [53]	High	Zero	Accurate	Fast	Moderate	Varies	High
BFO [54]	High	Zero	Accurate	Fast	Moderate	Varies	High
FPA [55]	High	Zero	Accurate	Fast	Moderate	Varies	High
GSA [56]	High	Zero	Accurate	Fast	High	Varies	High
FUZZY [57–61]	Moderate	Small	Accurate	Fast	High	Varies	High
ANN [62–66]	Medium	Small	Accurate	Fast	High	Varies	High

V- PV voltage, I- PV current, T- temperature, G- irradiation: varies – based on constrains use V, I, T, G

analysis of the benefits and limitations of these methods is provided in Table 4.

In a microgrid communication system, the continuous monitoring of real-time data is essential. This is necessary to ensure grid stability, enhanced energy management, detection and isolation of faults, data analysis and optimization through the predominant communication data. Therefore, it is crucial to continuously monitor real-time data such as solar, wind, battery and load parameters to manipulate energy management operations, balance power demand and minimize wastage. By utilizing communication systems, we can reduce operational costs and enhance grid reliability.

The communication system can be classified into two categories: wired and wireless technologies. Wired systems, including DSL, PLC and fiber optics, provide faster data transmission and higher reliability, albeit at a greater installation cost. In contrast, wireless systems such as Zigbee, GSM and IoT are more economical to implement, making them the preferred choice for remote locations. In a microgrid system, researchers working in rural areas prefer an IoT-based communication system [100–103]. Furthermore, some researchers [104–106] are implementing IoT-based energy management strategies, including demand response programs, to enhance the performance of microgrids and

Table 2 Comparison for WECS control method

Method	Benefit	Drawback
Pitch angle control [67]	Control power production efficiently when there is a high wind speed	Due to blade misalignment and mechanical deterioration in wind-driven vehicles, pitch angle adjustment can impair power output
Tip speed control [68, 69]	Regulates power production, balances energy supply and demand and lowers frequency variations to maximize power collection, safeguard turbines from over-speeding and improve grid stability. This makes sure that wind energy is effectively converted into electrical energy	Tip speed control reduces power production in low wind conditions, increases blade fatigue and wear and requires sophisticated algorithms and sensors for wind speed tracking and pitch angle adjustments, increasing system costs and maintenance requirements
Generator optimal torque control [70]	For optimum performance in varying wind conditions, it maximizes power production, improves energy capture and adapts to wind conditions	It necessitates sophisticated algorithms and sensors, putting strain on wind turbine parts and raising the possibility of power imbalances that might impair grid quality or stability
P & O [71]	Simple, low-cost implementation that works with several types of wind turbines	Losses, a delayed reaction to changes in wind speed, and a sensitivity to erroneous tracking are all results of oscillations around the power point
ICM [72]	Enhanced precision in monitoring, management of environmental situations, mitigation of the impact of partial shading and attenuation of oscillatory behavior	Number of sensors increased compared to P&O, complex control algorithms, computational demands, slow response to wind conditions
GA [73]	GA-based MPPT algorithms, through global optimization, can efficiently identify the maximum power point in wind energy systems without needing a specific mathematical model, and can adapt to changing conditions and be implemented in parallel for optimal efficiency	Proper tuning of algorithm parameters is essential for effective performance, which may necessitate expertise and extensive experimentation, while GA-based algorithms might converge slowly due to needing a large number of iterations, especially in dynamic or noisy environments, and the performance of GA-based MPPT algorithms can be affected by initial population settings and genetic operators, potentially leading to suboptimal solutions if not properly initialized or tuned
PSO [74]	PSO-based MPPT algorithms provide effective global optimization and can adjust to changing environments	Algorithm might face challenges such as restricted exploration in intricate terrains, early convergence, parameter sensitivity and getting stuck in local optimal solutions
CC [75]	Cuckoo search-based MPPT algorithms for wind energy conversion systems are designed to efficiently optimize globally by imitating the parasitic behavior of cuckoo birds. They demonstrate rapid convergence rates and can accurately locate the maximum power point (MPP) across different wind conditions	They might face challenges in intricate solution landscapes, potentially resulting in premature convergence and less than optimal solutions. Moreover, fine-tuning parameters is essential for achieving peak performance, as the sensitivity to parameter configurations could influence the algorithm's effectiveness
GWO [76]	Grey Wolf Optimization (GWO)-based MPPT algorithms utilize the grey wolves' hunting behavior to efficiently locate the maximum power point (MPP) in intricate solution spaces. These algorithms show quick convergence and excellent global optimization abilities, proving to be effective in various wind conditions	GWO algorithms might be sensitive to parameter configurations, necessitating precise adjustments for optimal performance. Furthermore, they could encounter challenges in dealing with solution landscapes that have multiple modes, which could potentially result in less than optimal solutions
Fuzzy logic [77]	Proficient in managing uncertain and imprecise wind conditions. It integrates linguistic variables and regulations to capture subjective wind speed, which in turn facilitates precise monitoring of the highest power points	Fuzzy logic controller design and tuning is difficult and time-consuming, requiring accuracy and knowledge of wind energy systems. Performance might suffer in unfamiliar wind conditions due to poor generalization and inadequate representation
ANN [78]	These algorithms are capable of adjusting to varying wind conditions and effectively managing nonlinear system dynamics. ANN algorithms show rapid convergence and have the ability to understand intricate connections between input variables and the best power output level	ANN demands substantial computational resources during training and may encounter overfitting issues if not trained properly

Table 3 Comparison of different controller for BESS

Bidirectional converter controller	Benefit	Drawback
PI [79]	Control algorithm that is widely used and well understood, Excellent steady-state and transient responsiveness It is simple to adjust for diverse system dynamics. Implementation is rather straightforward	Inability to deal with nonlinear systems and uncertainty Manual adjustment may be required for best performance Variations in system parameters can have an impact on performance
PID [80]	The enhancement of dynamic response and robustness in controlling battery bidirectional converters results in improved system performance	PID controllers are characterized by a higher level of complexity in both design and implementation when compared to PI controllers, necessitating a greater allocation of computational resources and specialized knowledge
Single phase shift [81]	The design of converters decreases the number of components required, resulting in cost reduction This approach improves the efficiency of the system by reducing switching losses commonly linked to traditional PWM control	Limited control flexibility, in comparison to more intricate modulation methods, can result in decreased performance when faced with fluctuating load conditions caused by a fixed phase shift
Extended phase shift [82]	It allows for a more precise regulation of power distribution, leading to increased efficiency and quality of power conversion This method demonstrates superior operational capabilities in response to fluctuations in load compared to employing single phase shift control	The creation and execution of controllers could result in elevated expenses and demands for resources The utilization of extended phase shift control might bring about extra switching losses and harmonic distortions, necessitating meticulous optimization
Dual phase shift [83]	It enables improved power flow balancing and reduced ripple in battery bidirectional converters, ultimately enhancing the overall stability of the system This approach provides greater flexibility and precision in control when compared to single phase shift techniques, particularly in managing uneven loads	Control can lead to a higher level of intricacy in the development and execution of controllers, which could potentially lead to elevated costs and necessitate specialized knowledge The requirement for accurate adjustments to the phase angle may pose difficulties in attaining optimal performance in fluctuating operational scenarios
Fuzzy logic [84, 85]	Capability to deal with nonlinear systems and uncertainty Can efficiently capture expert knowledge and language rules Provides durability and versatility Capable of handling complicated control settings	Difficult to tune and optimize the fuzzy rules Increased computational complexity compared to other controllers May require a large rule base to achieve desired performance A broad rule base may be required to get the necessary performance
Sliding Mode Controller [86]	Robustness to changes in and disturbances to parameters Rapid dynamic responsiveness and precise tracking Simple tweaking and installation procedures Suitable for highly unpredictable and nonlinear systems	Electrical noise and high-frequency switching There may be a chattering phenomenon, which puts more strain on the system's parts Sensitivity to errors in system modeling In order to balance performance and chattering, careful tweaking may be necessary
Model predictive control (MPC) [87]	It demonstrates enhanced efficacy in monitoring specified operational settings and managing limitations in battery bidirectional converters It allows for adaptability in enhancing various objectives concurrently, including efficiency, power quality, and system stability	It can be difficult to acquire in real-world scenarios. MPC necessitates significant computational power and immediate fine-tuning, which could result in increased expenses and intricacy

Table 4 Comparison of different control methods for EMS

Methods	Benefit	Drawback
Linear And Nonlinear Programming [88, 89]	The Micrgrid combines power sharing, continuous run and on/off modes Minimize operating costs of conventional generators (CGs), while adhering to droop controlled active and reactive power dispatch constraints	It is essential to evaluate the impact of depth of discharge (DOD) on battery efficiency, greenhouse gas emissions of conventional generators on the environment, privacy concerns of customers, integration of demand response (DR) and the reliability of the system
Dynamic programming [90, 91]	The objective function includes the operational cost of CGs and penalty cost on load shedding, with the Pontryagin maximum principle utilized to reduce computational time; Selecting a higher DOD accelerates battery degradation, while DR is not factored in the centralized forecasted cash flow minimized by minimizing energy trading cost with the main grid and battery aging cost	A significant amount of effort is needed to address environmental pollution, incorporate demand response, and address privacy concerns in optimizing microgrid systems
Rule-based methods [92, 93]	The power balancing of building integrated microgrids is maintained along with stabilization of DC bus voltage The central EMS overseeing the energy operation of the entire microgrid and the prosumer EMS handling power imbalances in the prosumer system	Generation of renewable energy resources, voltage regulation of MG system, operation cost, energy transaction cost and DR are all excluded from consideration
Matrix real coded genetic algorithm [94]	Smart EMS model, where distributed energy resources marginal price bids are utilized to reduce the operational cost of Microgrid	The emission cost of microturbine and DR are not being taken into account
Particle Swarm Optimization [95]	EMS uses a power offering strategy based on PSO to minimize costs and coordinates DERs to minimize power fluctuations, aiming to optimize revenue for Virtual Power Plant	The minimization of power peaks is a recently established goal, while the maximization of profit within the energy market is deemed crucial
Slime mold algorithm [96, 97]	This research delves into optimizing the performance of an independent microgrid by integrating the demand response program (DRP) to enhance energy management efficiency and reduce costs and emissions A rapid methodology decreases operating costs and emissions by utilizing various renewable sources	Challenges arise from fluctuations in unpredictable renewable energy sources and varying energy consumption levels
Cockroach swarm algorithm [98]	A cost-effective microgrid-based energy management system was created for off-grid and on-grid systems with solar PV generation and batteries, utilizing an improved cockroach swarm optimization technique for daily cost analysis	Conflicting interests of builders and future residents are reconciled through optimization to address challenges in the optimal installation of energy components in residential complexes
Gravitational search algorithm [99]	The operating expenses of a standalone microgrid are reduced by taking into account three different situations: regular operation, peak electricity demand and the ability to easily connect new components	High depth of discharge (DOD) results in a rapid decline in battery lifespan. The environmental impact of carbon generation is not taken into account

achieve energy and cost savings. Based on the observation, this system includes energy monitoring to optimize microgrid operation, enabling remote management through the internet and improving energy management. This benefits both consumers and power companies.

In this section, recent work on a small-scale microgrid is reviewed to identify research gaps for my proposed work. In [107] the author suggests a small-scale system using a traditional MPPT algorithm, but one notable advancement in the experimental setup is the rapid control prototyping model for testing various control algorithms in future. In the same author's work, a rule-based EMS is developed, although a traditional MPPT method is utilized. In [108] the author incorporates WECS and PVES, proposing the gain scheduled proportional integral controller in the paper. In [109] the author conducts real-time control using rapid control prototyping to experimentally test and validate the control algorithms of the microgrid system. Another author [110] focuses on an energy management strategy that regulates the

energy flow between the hybrid microgrid system and the loads connected directly or to the utility grid.

Based on the literature review, it is apparent that small-scale microgrids necessitate highly efficient control algorithms for fully leveraging the potential power generation of hybrid systems. Furthermore, a dependable monitoring and management system is essential for maintaining the performance of the microgrid. Additionally, in hybrid setups, having a battery backup with a sophisticated charging controller is crucial to maintain power equilibrium when dealing with fluctuating load and generation scenarios.

In this research, ANN-based MPPT algorithm is proposed in the solar and wind energy conversion system controllers and also battery storage system. Furthermore, to improve the performance of ANN controller the two major key issues such as significant training data and hyper parameter (hidden layer and initial weight) will be resolved in this work. For example, the real-word data are collected from NASA Research Center System as depicted in Fig. 2 and trained the neural network properly to avoid overfitting and the rapid variation of input variables the accurate output will produce in controller because of significant data will trained in ANN. Generally, the neural network initial weigh and bias of the network are generated by back-propagation algorithm and number hidden layer value set by user. Such algorithm is susceptible to getting trapped in local optima, especially for complex problem with high-dimensional data. This issue is resolved by grey wolf optimization algorithm which is applied in ANN to generate optimized value of the initial weight and number of hidden layer. This optimized ANN parameter avoids the local optima trapped and produces the very minimum mean square error value, so it improves the performance of ANN to predict the optimal output value. In this work an IoT-based wireless communication system has been implemented in a small-scale microgrid system to efficiently monitor real-time data including the values of wind, solar and battery parameters. Additionally, a simple and intelligent battery state of charge rule-based system, along with an IoT-integrated energy management system, is established for small-scale microgrid systems. This system is designed to balance power demand and minimize power generation wastage and maintain.

1.1 The summarization of this research work constitutes its primary contribution

- The proposed MPPT techniques aim to optimize the power output of each generating unit, encompassing both the wind-driven generator (WDG) and the PV array.
- GWO-tuned ANN controller is implemented for a BESS converter to retain the DC bus voltage to a constant magnitude during different sudden disturbances in energy sources and load.

- IoT-based wireless communication system is implemented.
- Microgrid performance will be enhanced through the deployment of an intelligent energy management system.

This document is organized as follows: In a beautifully detailed way, Section 2 provides a comprehensive depiction of the complete system design, converter topologies and control techniques in an elaborate manner. Section 3 covers the test system, including multiple case studies and Simulation results. Section 4 describes experimental validation and results, followed by conclusions in Sect. 5.

2 System description

The proposed small-scale microgrid that has been suggested is made up of a system that preserves solar energy, another one that preserves wind energy, and a remarkable storage system for battery energy. Each conversion system contains conventional converters, and a unique regulated algorithm has been created. The entire works are synchronized and monitored by the intelligent energy management system that has been proposed, as demonstrated in Fig. 3.

2.1 Solar power generation system (SPGS)

Solar power generation system as depicted in Fig. 4 encompassed of PV arrays, conventional boost converter [34–42] and proposed controller. The solar panel arrays convert light energy in to electrical energy and boost converter to boost the solar panel voltage for desire load application with help of controller. A 500 watts solar panel is used for in this work and utilized the maximum power with help of optimized ANN controller which is implemented for conventional boost converter. The various ecological conditions the suggested controller to track the extreme power effectively and generate the optimum Vref value, then it will compare with actual PV voltage it generate error signal after that is goes through PI controller it generate optimized duty cycle for boost converter.

In addition to turn on and off by MPPT controllers based on battery SOC condition, if the microgrid system is satisfied, the load constraints and the hybrid sources generate the excess power and the battery will charge continuously; if the battery SOC increases the above boundary condition, it will affect the battery components, so avoid this circumstance of the MPPT controller turn on and off by SOC boundary condition; once the battery SOC reaches the upper limit, the MPPT controller automatically turns off, for this effective operation to reduce the battery stress and increase the lifespan of battery as shown in Fig. 4. 500W solar panel P–V and
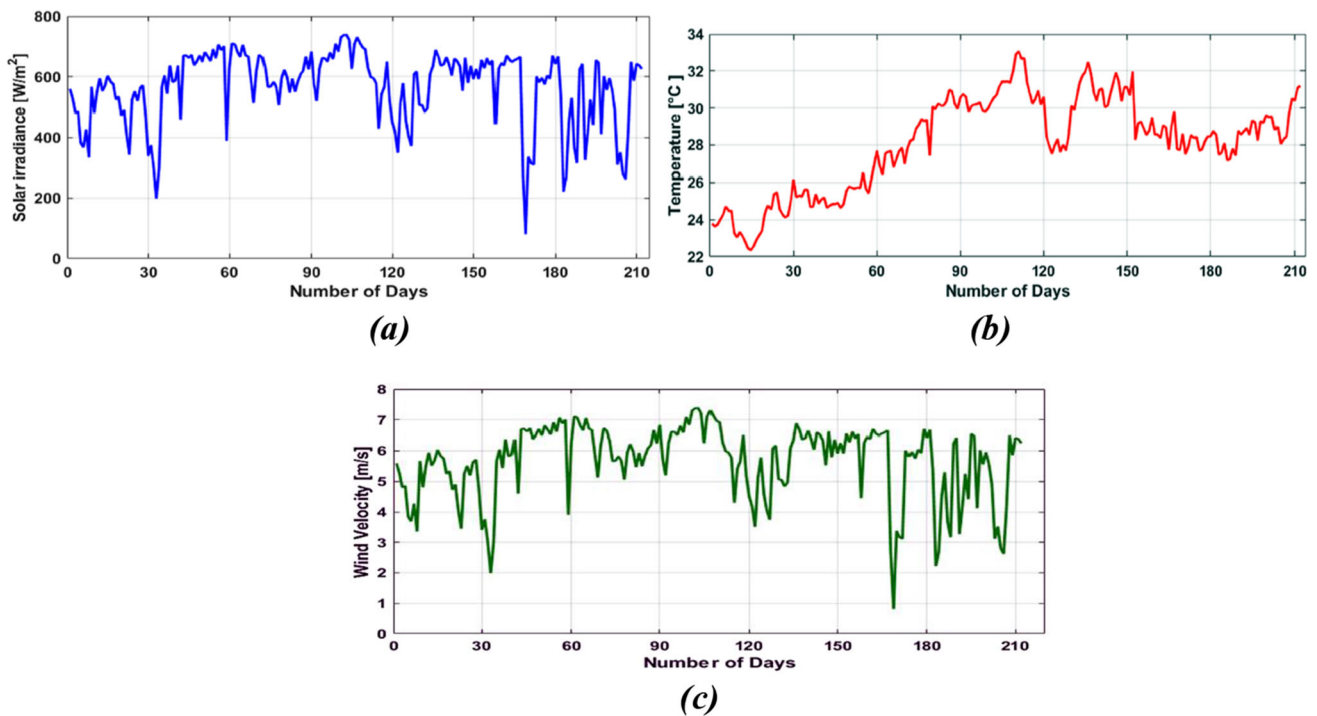
Fig. 2 Real word data: **a** solar irradiation, **b** Temperature, **c** wind velocity

I–V characteristics with the effect of irradiance are shown in Fig. 5. It is apparent from the aforementioned graphical depictions that the solar panel exhibits a nonlinear behavior with respect to both voltage and current as the irradiance changes. The properties are displayed for various levels of irradiance that span from 250 to 1000 W/m² while retaining a persistent temperature of 25 °C and various levels of temperature that span from 25 to 40 °C while retaining a constant 1000 W/m² irradiance level. An output power of 500Wp is measured at 12 V at a maximum irradiance level of 1000 W/m².

2.2 Wind power generation system

The power generated from wind is determined by various factors. Especially, "it is derived using the air density (ρ), the surface area swept by the rotor blades (A) and the velocity of the wind (v)" [67]. The power coefficient, denoted as Cp, is also taken into consideration and is influenced by the tip speed ratio (TSR) and pitch angle. In this particular system, a wind turbine with adjustable speed is utilized and the attributes of this turbine can be witnessed in Fig. 6, which exhibits the Cp values for various wind speeds and pitch angles [67–70].

$$P = \frac{1}{2} * \rho * A * v^3 * C_p(\lambda, \theta) \qquad (1)$$

The wind power generation system contains a turbine coupled generator setup used to generate AC power, and it depends on wind velocity. After that, the three-phase AC supply undergoes conversion into DC through a diode bridge rectifier and then increases the rectifier voltage level with support of DC–DC boost converter. To extract the maximum power in WECS here, the GWO-tuned ANN-MPPT controller implemented to generate the optimum pulse width for DC–DC boost converter is shown in Fig. 7.

2.3 Battery energy storage and management system

The BESS comprises a lead acid battery, a DC–DC bidirectional converter [79] and a proposed controller, as illustrated in Fig. 8. The charging process is contingent upon the surplus power produced by renewable energy resources, while the discharging process hinges on the load and the absence of RES. In the proposed work the battery reference current is generated by ANN controller and the controller hyperparameter is optimized by grey wolf optimization method; the design and implementation process is mentioned in detail in flowchart as shown in Fig. 10. After getting the reference current, it will compare actual battery current and then the signal goes to PI controller; it produces optimized pulse width of the bidirectional DC–DC converter. Equations (2) and (3) offer the explanations for the battery's state of charge (SOC) and
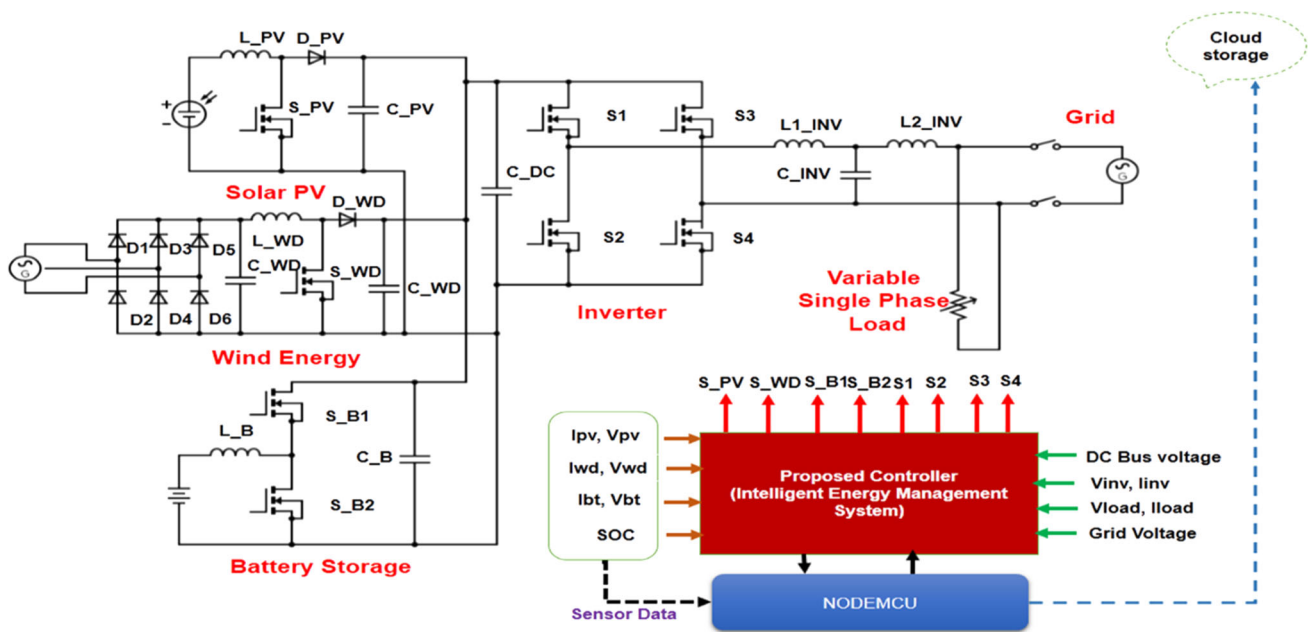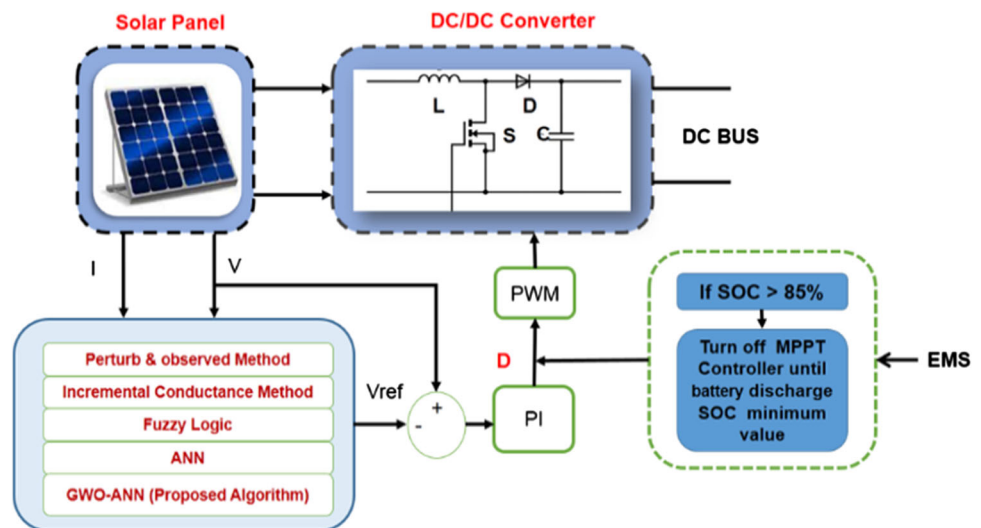
Fig. 3 The proposed small-scale microgrid system

Fig. 4 The proposed solar energy conversion system with controller

its corresponding limits.

$$SOC = 100 * \left(1 + \frac{\int I_{bat} dt}{Q}\right) \quad (2)$$

$$SOC_{min} \leq SOC \leq SOC_{max} \quad (3)$$

Furthermore, the performance of BMS is decided by battery state of charge (SOC) constraints. This research adheres to several key measures for an effective battery management system. Firstly, if the battery SOC limit reaches the upper boundary value, the solar controller algorithm is turned off, and the determined power is delivered by the battery until the SOC value decreases to the lower boundary limit. Secondly,

if the battery SOC limit reaches the lower boundary limit, the battery is only in charging mode, and if the generation also decreases at the same condition, load scheduling is done by EMS system.

2.4 Grey wolf optimization algorithm

The GWO method takes motivation from the hunting behavior of grey wolves, who operate in a four-level hierarchy to capture their prey [111]. The alpha (α) leads the group and is responsible for making all decisions related to the hunt. The beta (β) supports the alpha in decision-making and holds a sub-leadership position. The delta (δ), the third tier of the hierarchy, must obey the alpha and beta but have authority

(a)

(b)

(c)

(d)
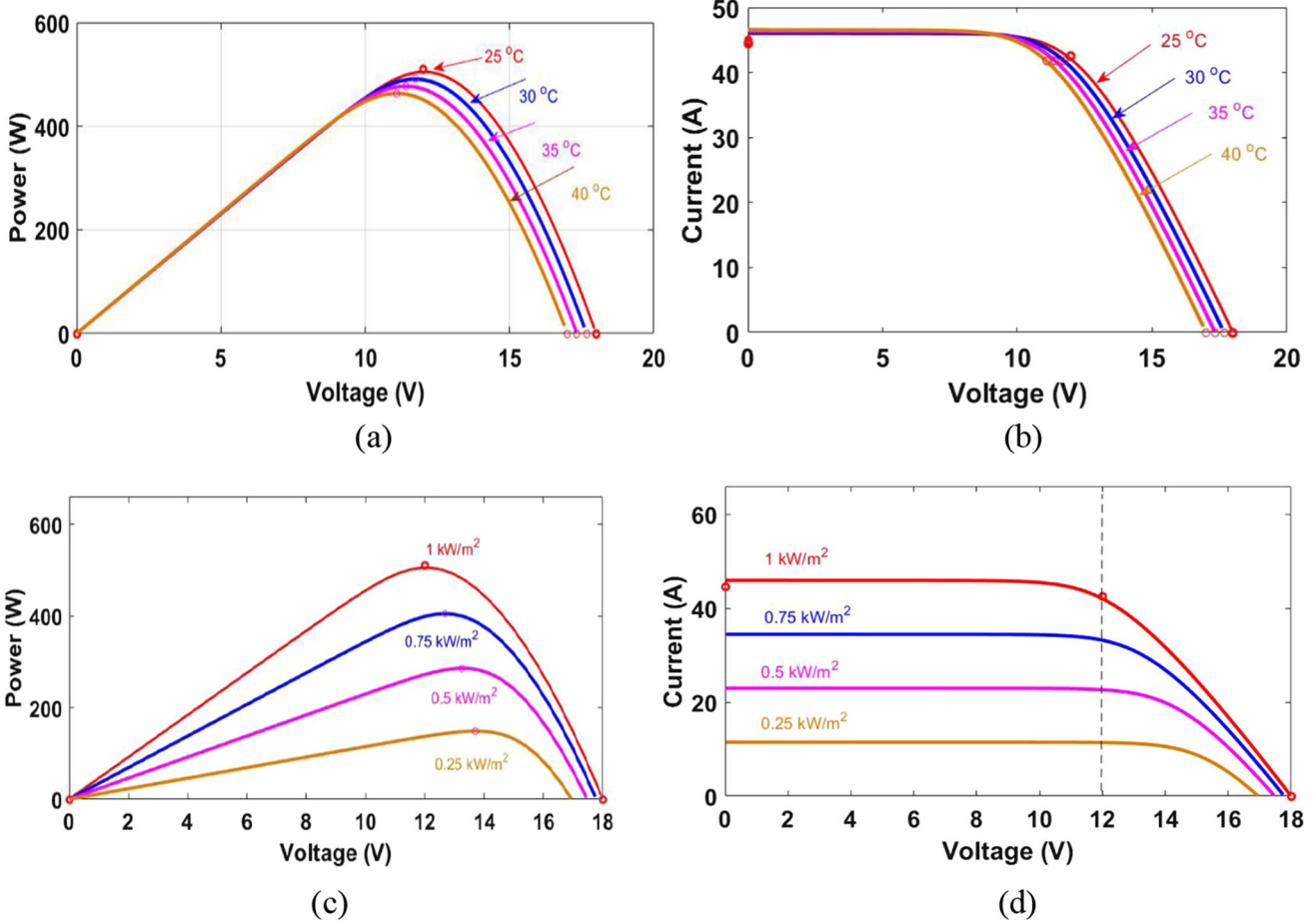
Fig. 5 500W PV module P–V and I–V characteristics under different situations: **a** and **b** show variations in values of temperature (T) while maintaining a constant irradiance (G) of 1000 W/m^2; **c** and **d** demonstrate variations in irradiance (G) while keeping the temperature (T) constant at 25 °C

Fig. 6 The wind turbine mechanical attributes in relation to various wind velocities
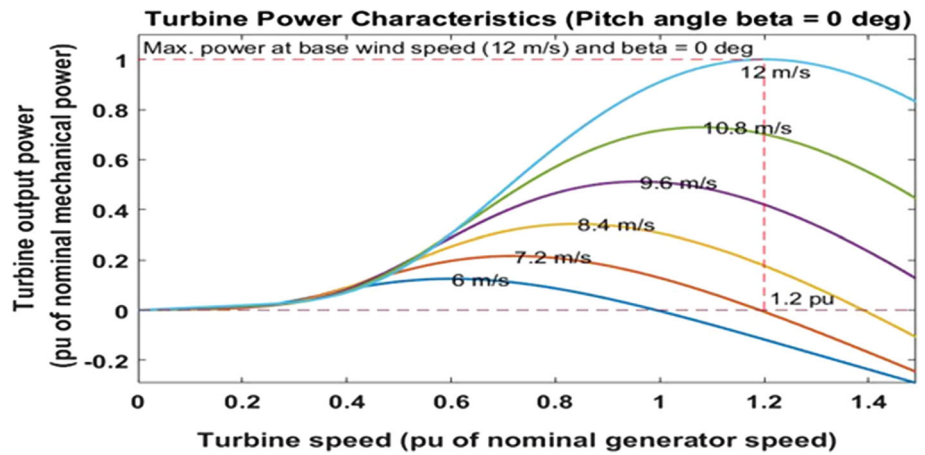
Fig. 7 The proposed wind power generation system
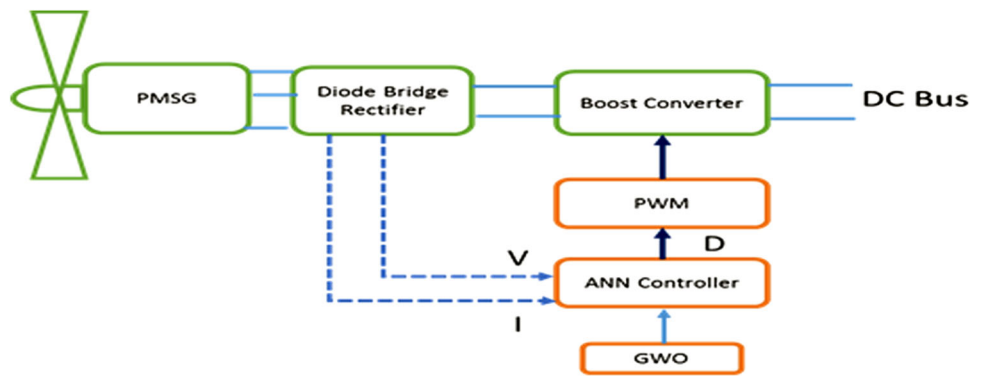
Fig. 8 The proposed battery energy storage and management system
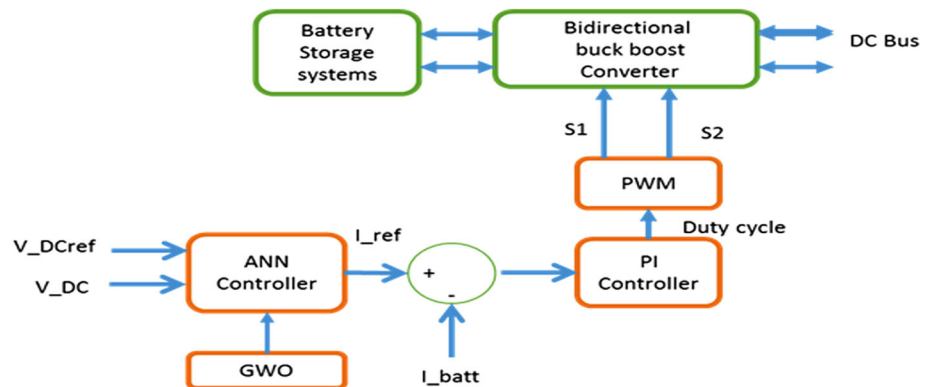
over omega (ω), the lowest rank in the pack, which must submit to all higher-ranking wolves. The GWO algorithm partitions possible solutions into four distinct categories in order to replicate the hierarchical structure of leadership. The highest-rated solution is known as alpha, the second best as beta, and the third best as delta, while any remaining solutions are designated as omega. The process of hunting involves the encirclement of prey by grey wolves, and this particular stage can be accurately represented through the utilization of mathematical Eqs. (4)–(7).

$$\overrightarrow{H} = \left| \overrightarrow{C}\,\overrightarrow{X}(t) - \overrightarrow{X}(t) \right| \tag{4}$$

$$\overrightarrow{X}(t+1) = |\overrightarrow{X}_p(t) - \overrightarrow{A}\,\overrightarrow{H}| \tag{5}$$

$$\overrightarrow{A} = 2\overrightarrow{a}\,\overrightarrow{n_1} - \overrightarrow{a} \tag{6}$$

$$\overrightarrow{C} = 2\overrightarrow{n_2} \tag{7}$$

When referring to the current iteration, t, the position vectors of a search agent $\overrightarrow{X}$ and the optimal solution $\overrightarrow{X}_p$, also known as the prey position, are taken into consideration. Additionally, coefficient vectors $\overrightarrow{A}$ and $\overrightarrow{C}$ can be computed using the equations provided. During the iterations, the components of vector $\overrightarrow{a}$ are gradually decreased in a linear

manner from 2 to 0, while vectors $\overrightarrow{n_1}$ and $\overrightarrow{n_2}$ are randomly selected from the range of 0 to 1.

During the hunting phase, α, β, and γ are responsible for conducting the operation due to their superior understanding of the probable location of the optimal solution. Other search agents are required to modify their locations by considering the position of the most optimal search agent. To achieve this, the location of the search agent can be adjusted as follows in Eqs. (8)–(12).

$$\overrightarrow{H_a} = \left| \overrightarrow{C_1}\overrightarrow{X_\alpha}(t) - \overrightarrow{X} \right| \tag{8}$$

$$\overrightarrow{H_\beta} = \left| \overrightarrow{C_1}\overrightarrow{X_\beta}(t) - \overrightarrow{X} \right| \tag{9}$$

$$\overrightarrow{H_\gamma} = \left| \overrightarrow{C_1}\overrightarrow{X_\gamma}(t) - \overrightarrow{X} \right| \tag{10}$$

$$\overrightarrow{X_1} = \left| \overrightarrow{X}_\alpha - \overrightarrow{A}\,\overrightarrow{H_\alpha} \right|; \ \overrightarrow{X_2} = \left| \overrightarrow{X}_\beta - \overrightarrow{A}\,\overrightarrow{H_\beta} \right|; \ \overrightarrow{X_3} = \left| \overrightarrow{X}_\gamma - \overrightarrow{A}\,\overrightarrow{H_\gamma} \right| \tag{11}$$

$$\overrightarrow{X}(t+1) = \frac{(\overrightarrow{X}_1 + \overrightarrow{X}_2 + \overrightarrow{X}_3)}{3} \tag{12}$$

The GWO algorithm is able to seamlessly transition from exploration to exploitation by utilizing adaptive values for search and attack of prey, represented by $\overrightarrow{a}$ and $\overrightarrow{A}$. During

the exploration phase, half of the iterations are dedicated to exploring and seeking out prey by decreasing $\overrightarrow{A}$ and ensuring that |A| is greater than 1. Conversely, during exploitation, the other half of the iterations are focused on attacking prey by setting |A| to less than 1.

2.5 ANN controller

In common a feed-forward neural network is comprised of three layers, namely input, hidden and output layer [112], as illustrated in Fig. 9. The mathematical definition of the dispersed dispensation system is represented by Eq. (13).

$$L = \sum_{J=1}^{n} W_{IJ} X_J + b_J \tag{13}$$

To effectively train a feed-forward artificial neural network (ANN) system, it is crucial to possess several key elements: the input training node xj, the associated connection weights wij for input, hidden and layer nodes, the bias bj for hidden and output layer nodes, and the total number of input signals, denoted as n [112]. The widely used method for this training process is the back-propagation (BP) algorithm. This algorithm, a sophisticated gradient technique, elevates the performance of the ANN by iteratively adjusting the weights and bias terms of each node. This iterative process continues until the output value at the output layer accurately predicts the desired outputs, thereby minimizing the training error. Fundamentally, the mean-squared error (MSE) acts as the cost function, which can be mathematically represented by Eq. (14).

$$MSE = \frac{1}{n} \sum_{i=1}^{n} \sum_{j=1}^{m} [L_j(i) - T_j(i)]^2 \tag{14}$$

where 'n' denotes the quantity of input data, 'm' signifies the number of output signals. '$L_j(i)$' represents the factual yield while '$T_j(i)$' indicates the target output [112, 113]. During the process of work, there are two control parameters that enhance the recital of the system, namely the initial weight for training nodes and the value of the hidden layer. Generally, the user sets the values of the hidden layer, while the initial weights are produced by the BP algorithm. But the usage of back-propagation algorithm for generating initial weight values in neural networks has certain drawbacks. Inadequate initialization may impede convergence, resulting in suboptimal solutions or local minima. It does not thoroughly explore weight space, thereby limiting generalization. Furthermore, the decision of weight values impacts other hyperparameters, making the tuning process complicated. Symmetric weights can decelerate learning, while imbalances may result in gradient issues. It necessitates resource-intensive trial-and-error

to determine appropriate values. The transfer to new tasks is a challenging process, and random initialization lacks control over weight distribution. Finally, uncertainty estimation is not provided.

2.6 GWO-ANN algorithm

As early said, the standard approach to initializing neural networks employs the back-propagation algorithm to generate initial weights and biases, while the user determines the number of hidden layers. Despite its susceptibility to local optima, this algorithm is still useful for handling intricate issues that involve high-dimensional data. To tackle these concerns in this research, the grey wolf optimization algorithm is employed in order to ascertain the preliminary weight and concealed layer variables of the artificial neural network (ANN). Thus, we have implemented a proposed control algorithm which has the capability to precisely assess the growth of neurons in the hidden layer without any prior selection by the user and locate optimized initial weight values. Our belief is that this method will greatly elevate the efficiency and precision of the ANN model through the enhancement of convergence rate and reduction of training error. Our research has effectively obtained a neural network with one output and two inputs for the hidden layer while achieving the lowest training error. Figure 10 illustrates the sequence of tasks involved in GWO-ANN, as represented by the flowchart.

2.7 Energy management system (EMS)

The microgrid solution is a complicated interconnected network that necessitates exact and synchronized management to guarantee efficient and dependable operation. The energy management system (EMS) serves as the primary controller, overseeing and coordinating all control actions. It plays a crucial role in managing and directing these actions. The ongoing research focuses on an intelligent EMS responsible for regulating various converter controllers that operate based on the EMS control mode. One example of such a controller is the non-isolated boost converter in the solar energy conversion system, which can function in either MPPT mode or off-MPPT mode depending on power generation and battery SOC limits. Similarly, the battery bidirectional converter can either charge or discharge and keeps the DC bus voltage constant. The wind energy conversion system's DC–DC boost converter operates in boost mode. However, ensuring power balance in the microgrid under various power generation and load demand conditions is a major challenge and it is represented by mathematical Eq. (15).

$$P_{Solar} + P_{Wind} - P_{Battery} - P_{Load} = 0. \tag{15}$$
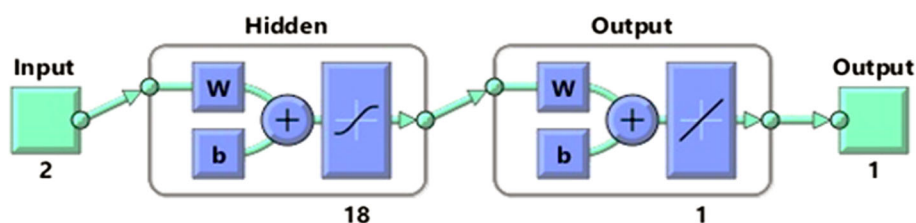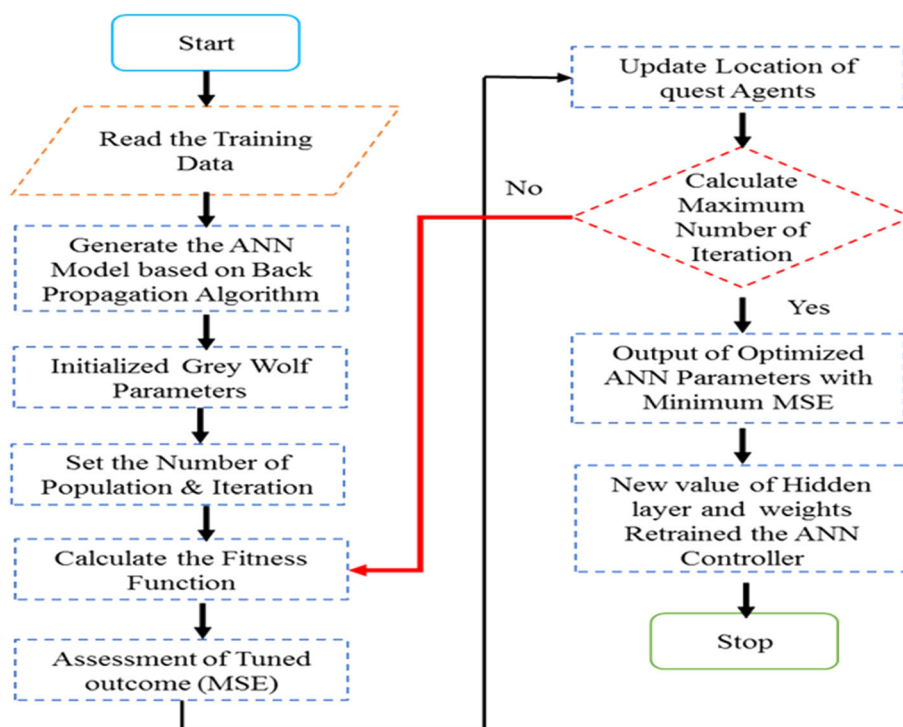
Fig. 9 General block diagram of ANN

Fig. 10 Flowchart for GWO-ANN Method

Any discrepancy between the power produced and the power utilized will result that there is a dissimilarity in voltage and frequency within the microgrid, thereby potentially causing instability and harm to the constituent elements. Therefore, it is essential to maintain a balance between the power generated and consumed to guarantee the dependable and efficient operation of the proposed system. In energy management system (EMS), four distinct modes of operation are utilized. Initially, in grid-connected mode, the EMS primarily monitors the battery state of charge (SoC), while the load requirements are met by the grid. Secondly, in islanded mode, the EMS first evaluates power generation, battery capacity and load demands. If power generation exceeds the load demand, surplus power is utilized to charge the battery and transferred to the grid. In the third scenario, when power generation is insufficient to meet the demand, the EMS prioritizes maintaining the battery SoC within limits. If the battery SoC is above 20%, power generation is initiated to balance the load demand. If the battery SoC exceeds 80%, the solar panel maximum power point tracking (MPPT) controller is disabled, and the load is powered by the battery until the

SoC drops below 80%. Lastly, if the battery SoC falls below 20% and power generation is inadequate, load scheduling operations are employed to ensure microgrid stability. The flowchart depicted in Fig. 11 elucidates the various methods by which the energy management system operates.

2.8 Load side control and conventional grid

Maintaining voltage and frequency is essential in small-scale microgrid systems, and the inverter serves as the backbone of the system, playing a vital role in ensuring optimal performance in both operating modes (grid and islanded). In islanded mode, it is crucial for the inverter to maintain voltage and frequency to effectively transfer power through local distributed networks and maintain system stability. In a grid-connected setup, the inverter guarantees synchronization of output voltage and frequency with the grid's standard rating. It also manages power flow control among hybrid sources, storage systems and the primary grid.
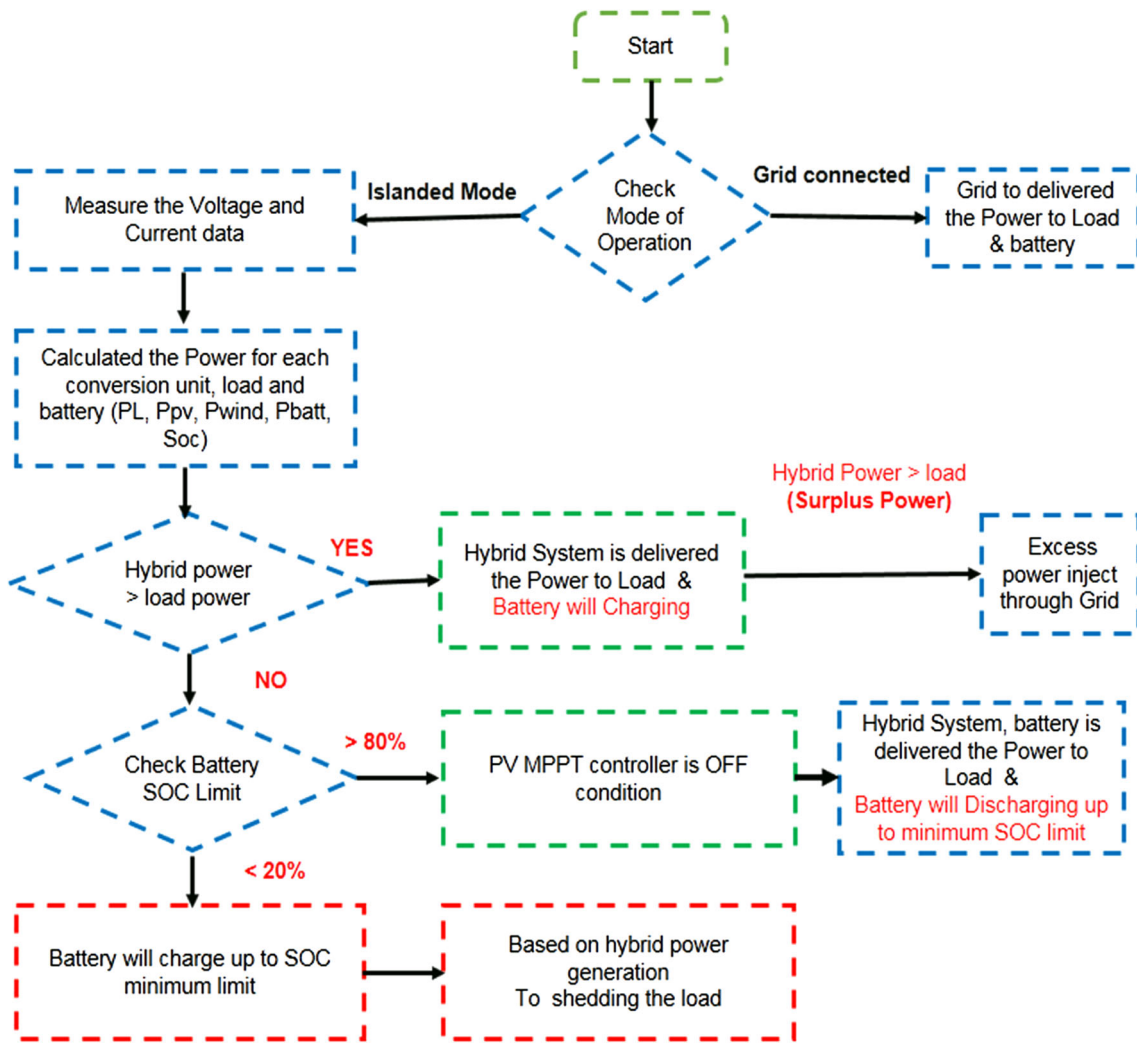
Fig. 11 Flowchart for intelligent energy management system
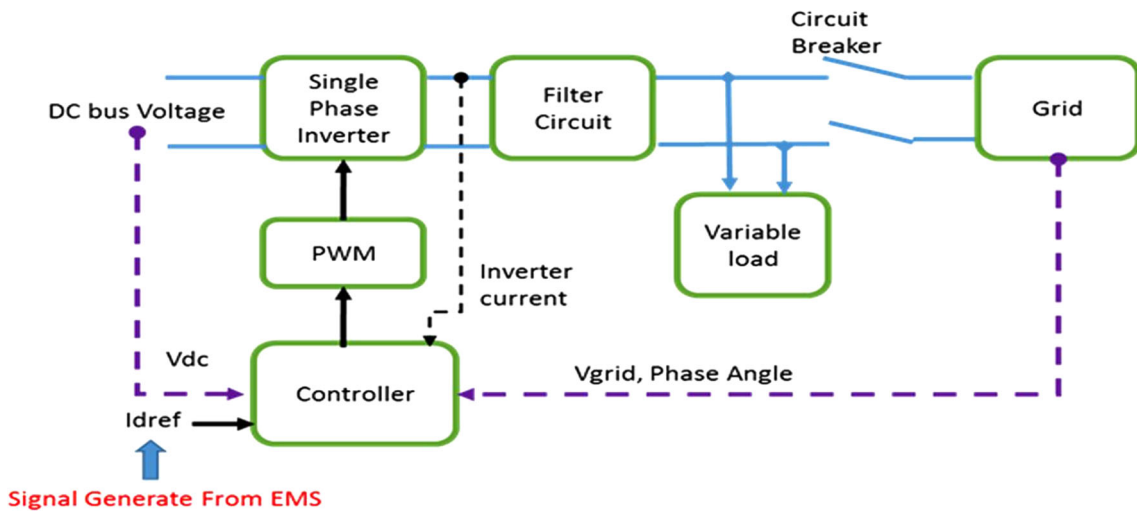
Fig. 12 Load side converter tie with Microgrid
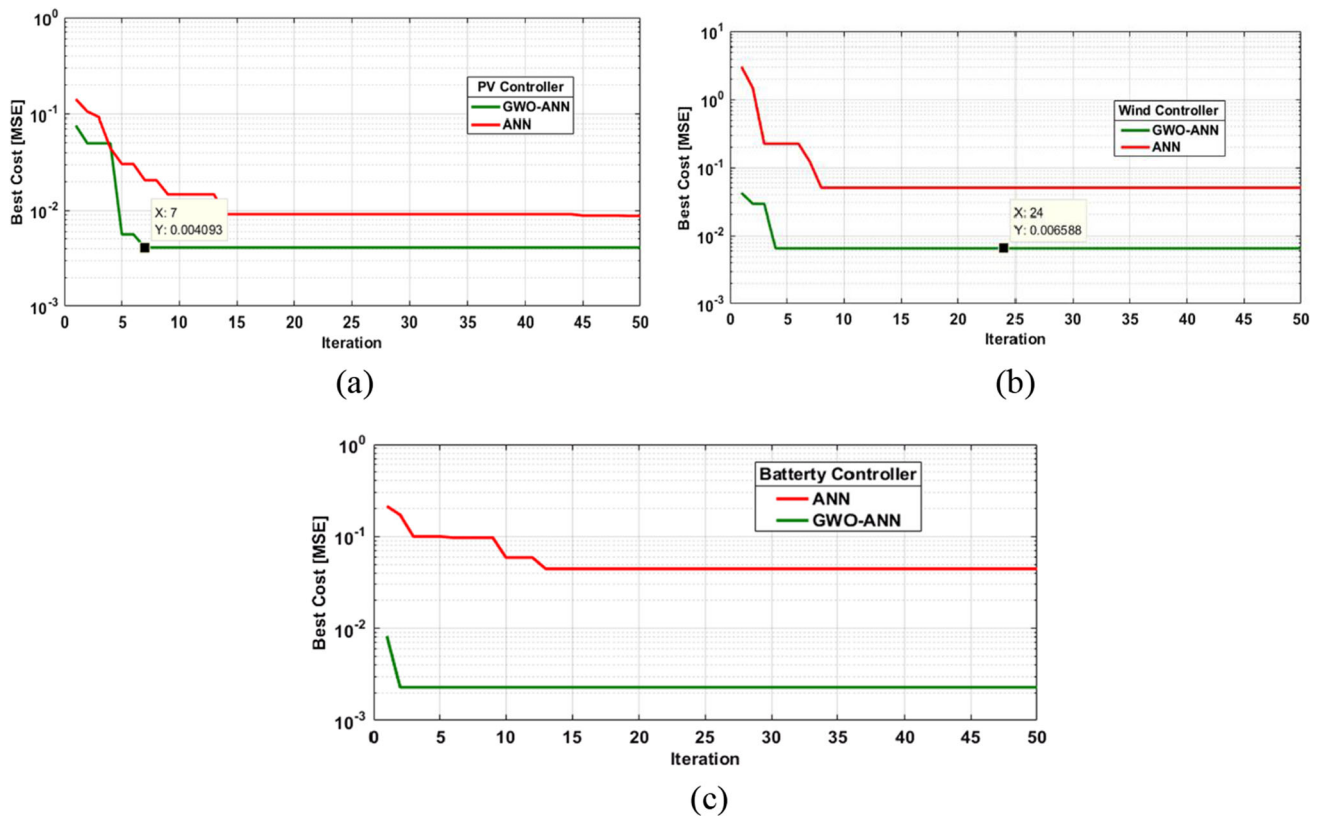
Fig. 13 Fitness values of proposed controllers. **a** PV, **b** Wind, **c** BMS

Managing power quality is also a significant task in this regard. To tackle this challenge, a simple yet effective controller has been devised for the inverter, as illustrated in Fig. 12. The load side control device comprises a variable load through a single phase grid-connected inverter and an LCL filter to reduce inverter output voltage and current harmonic. The inverter controller control parameter direct axis reference current value is generated by an intelligent energy management system due to the variation of hybrid generation and sudden changes in load.

3 Simulation result discussion

In this research, a microgrid framework configuration was conducted on a small scale and its performance was evaluated through the utilization of the MATLAB software. The initial phase of this section involved the development and appraisal of the control strategies for the PV, wind and battery energy storage systems. An analysis was conducted to compare the aforementioned strategy with other conventional methods. Following that, the microgrid's output was analyzed in islanded modes, and the study also examined how the intelligent energy management system functioned under varying load and ecological conditions. This section provides a detailed discussion of the aforementioned activities.

3.1 GWO-Tuned ANN algorithm for initializing weights and hidden layer parameters

To initiate the process, begin by selecting the structure of the ANN model and then focus on optimizing its initial weight values. This method can be implemented by a hybrid GWO-ANN technique which has been developed using specific parameters for the GWO optimizer, including a population size of 20 and a maximum iteration count of 50. The values of weight and hidden layer in this algorithm have a scale between -0.9 to 0.9 and 10 to 20, respectively. After running the hybrid algorithm, optimized hyperparameters are obtained. The algorithm's search history can be found and compared with conventional ANN method as shown in Fig. 13. The optimized values acquired are subsequently employed to train an artificial neural network (ANN) model through the utilization of the 'nntool' command within the MATLAB software. The performance of the ANN model is significantly improved with the optimized training approach using real data, resulting in enhanced predictions than using traditional ANN. By reason of the lesser MSE and fewer epochs obtained by all conversion unit controller, as illustrated in Fig. 13, Table 5 provides basic statistical analysis of the algorithm proposed.

Table 5 The preliminary computation of statistics for the suggested method showcases its potential efficacy

Controller	Training data			ANN		GWO- ANN	
	Input 1	Input 2	Output	Structure	MSE	Structure	MSE
PV	V_{PV}	I_{PV}	V_{ref}	$2 \times 18 \times 1$	0.00978	$2 \times \mathbf{18} \times 1$	0.0040
Wind	V_{Wind}	I_{Wind}	V_{ref}	$2 \times 18 \times 1$	0.0500	$2 \times \mathbf{18} \times 1$	0.0065
Battery storage	V_{DC}	V_{DCref}	I_{b_ref}	$2 \times 18 \times 1$	0.0440	$2 \times \mathbf{18} \times 1$	0.0022

structure: $2 \times 18 \times 1$ it mention 2 input and 18 hidden layer neurons and 1 output

Optimized hidden layer values are shown in bold

3.2 Dynamic performance of PV and wind energy conversion system

The performance of the PV and wind energy conversion unit control algorithm is to be analyzed using the MATLAB Simulink framework. The traditional MPPT algorithm will be compared with the proposed work.

The PV configuration consists of a PV array, boost converter and load, with the array comprising five PV modules connected in parallel. Similarly, the wind energy system configuration includes a variable wind turbine, PMSG, diode bridge rectifier, boost converter and load. The main parameters of the PV array and wind energy system, used in the simulation are provided in Table 6.

During the simulation, the solar irradiance (G) experienced an unexpected drop from 1000 to 700 W/m^2 between 1 and 2 s, followed by an increase from 700 to 800 W/m^2 between 2 and 3 s, another increase from 800 to 900 W/m^2 between 3 and 4 s, and a final increase from 900 to 1000 W/m^2 between 4 and 5 s. Throughout this timeframe, the input temperature (T) remained unchanged at 25 °C. According to the results shown in Fig. 14a, the exceptional predictive capability of the proposed GWO-tuned artificial neural network (ANN) method was clearly demonstrated in various atmospheric conditions, thanks to its highly optimized training strategy. After reaching the MPP, a comparison was made between the proposed method and the conventional methods like ANN, ICM, FLC and P&O. The power outputs recorded were approximately 499.5 W, 495 W, 492 W, 490 W and 478 W, respectively, under a solar irradiation of 1000 W/m^2. By examining the magnified section of Fig. 14a, it becomes evident that the proposed ANN method exhibits the least amount of fluctuations around the MPP compared to the other methods under steady-state conditions.

This ultimately leads to a reduction in consumption time. Building upon these observations, a comprehensive analysis was conducted on the conventional methods and GWO-tuned ANN techniques, with a focus on their key characteristics for PV. This analysis is presented in Table 7 and Fig. 15. Lastly, the predictive PV power efficiency of the proposed method was compared to that of the conventional P&O, FLC and ANN techniques.
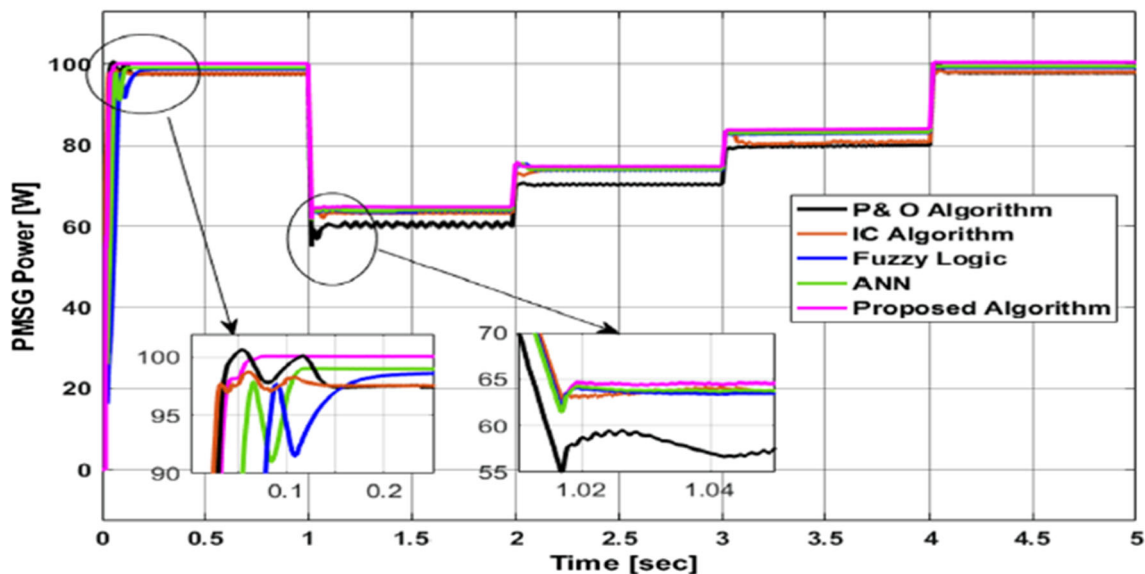
Table 6 PV and wind energy conversion system module properties

S. no.	Equipment	Parameter	Rating
1	PV model	Nominal power for single panel	100w
		Number of parallel connected strings	5
		Number of series connected strings	1
		Total Power	500 w
		V_{OC}	18 v
		I_{SC}	8.5
		V_{mpp}	12 V
		I_{mpp}	8.33 A
2	Boost converter	Inductor	0.461 mH
		Capacitor	556 μF
		Input voltage	12 V
		Output voltage	60 V
		Switching frequency	10,000 Hz
3	Wind	Nominal Power	100 W
		Nominal voltage	12 v
		Nomina current	8.4 A
4	Boost converter	Inductor	2.3 mH
		Capacitor	120 μF
		Input voltage	12 V
		Output voltage	60 V
		Switching frequency	10,000 Hz

Similarly, to analyze the performance of the wind energy system controller, only five distinct wind velocity values have been utilized in the proposed algorithm. These values were 12 m/s, 9 m/s, 10 m/s, 11 m/s and 12 m/s at the beginning, during the intervals of (0–1)s, (1–2)s, (2–3)s, (3–4)s and (4–5)s. Based on the findings in Fig. 14b, the proposed ANN method clearly demonstrated its exceptional predictive capability in various wind velocity conditions due to its highly optimized training strategy. Furthermore, it was determined to be remarkably robust in achieving the optimal maximum power point (MPP) under both increasing and
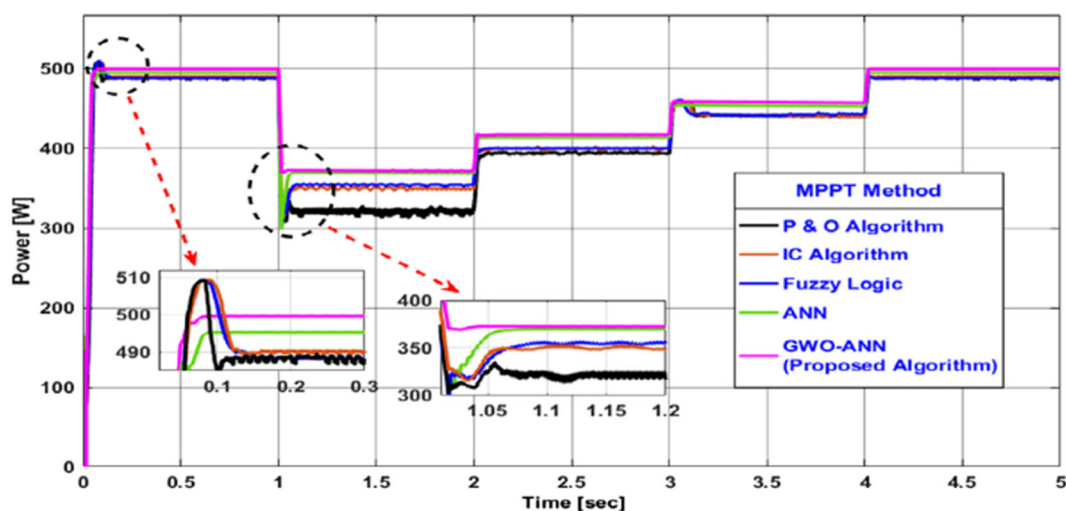
(a). The proposed method for solar energy conversion system performs better traditional methods in different solar irradiance level.

(b). The proposed method for Wind energy conversion system performs better than the traditional methods in different wind velocity conditions.

Fig. 14 **a** The proposed method for solar energy conversion system performs better traditional methods in different solar irradiance levels. **b** The proposed method for wind energy conversion system performs better than the traditional methods in different wind velocity conditions

decreasing levels of wind velocity. Comparing the GWO-tuned ANN method with the conventional methods ANN, ICM, FLC and P&O after reaching the MPP, the power outputs were approximately 99.78 W, 99 W, 98 W, 97.5 W and 97.4 W, respectively. The magnified section of Fig. 14b clearly demonstrates that the proposed ANN method exhibits the least amount of fluctuations around the MPP compared to other methods under steady-state conditions, resulting in reduced consumption time. Based on the observation, Table

8 presents a comprehensive analysis that was conducted on the traditional ANN, FLC, ICM, P&O control algorithm and optimized GWO-tuned ANN techniques, focusing on their key characteristics for wind. Additionally, Fig. 16 shows the comparison of the predictive wind power efficiency of the suggested method to that of conventional P&O, FLC and ANN techniques.

Table 7 A comprehensive analysis was conducted on the conventional method and GWO-tuned ANN techniques, focusing on their key characteristics for PV

Control algorithm	PV power (W)				Tracking Time (S)	Oscillation	Average efficiencies
	Solar irradiance [G] [W/m^2]						
	1000	900	800	700			
P&O	487	438	391	323	0.15	High	93.12
ICM	490	440	398	348	0.13	Medium	95.47
FUZZY LOGIC	492	442	400	352	0.08	Medium	96.06
ANN	495	454	413	365	0.05	Low	98.51
GWO-ANN	499.5	458	417	372	0.043	Very low	99.66

Fig. 15 The proposed method's predictive PV power efficiency was related to that of conventional techniques
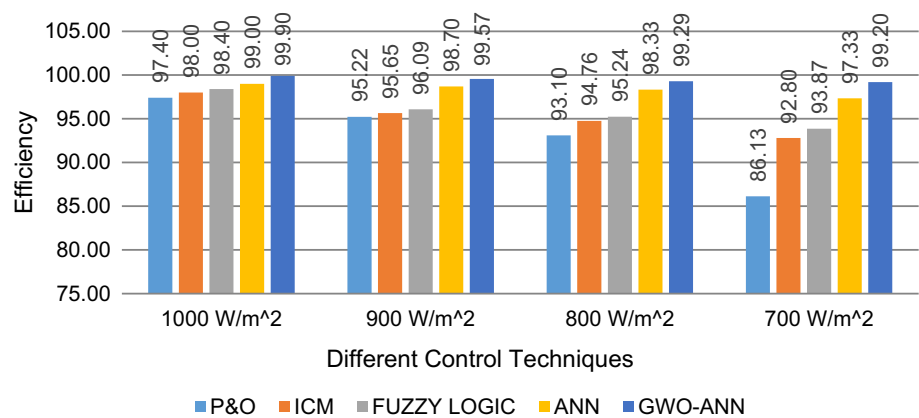
Table 8 A comprehensive analysis conducted on the conventional MPPT techniques and optimized ANN-MPPT techniques, focusing on their key characteristics for wind

Control algorithm	Wind power (W)				Tracking time (s)	Oscillation	Average efficiencies
	Wind velocity [m/s]						
	12	11	10	9			
P&O [71]	97.4	79.55	70.38	61	0.12	High	94.67
ICM [72]	97.5	80.93	73.42	63.37	0.10	Medium	97.02
FUZZY LOGIC [77]	98	82.61	73.78	63.56	0.08	Medium	97.84
ANN [78]	99	82.9	74.01	63.82	0.045	Low	98.35
GWO-ANN (proposed method)	99.78	83.73	74.69	64.73	0.040	Very low	99.36
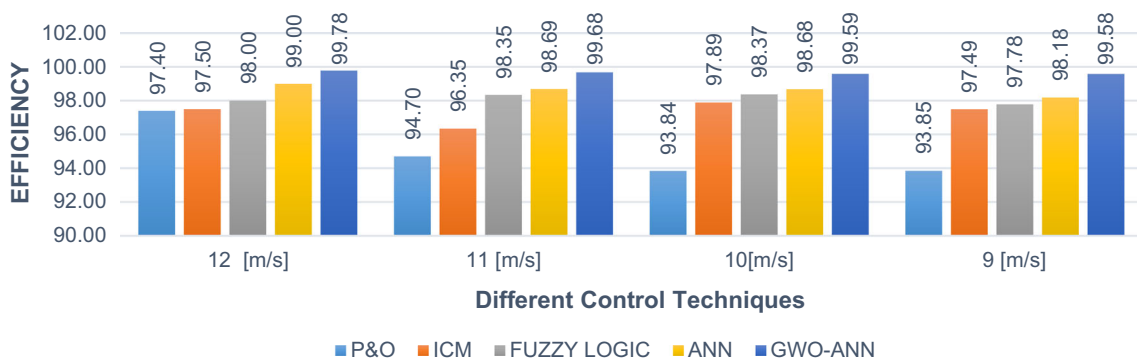
Fig. 16 The proposed method's predictive wind power efficiency was related to that of conventional techniques
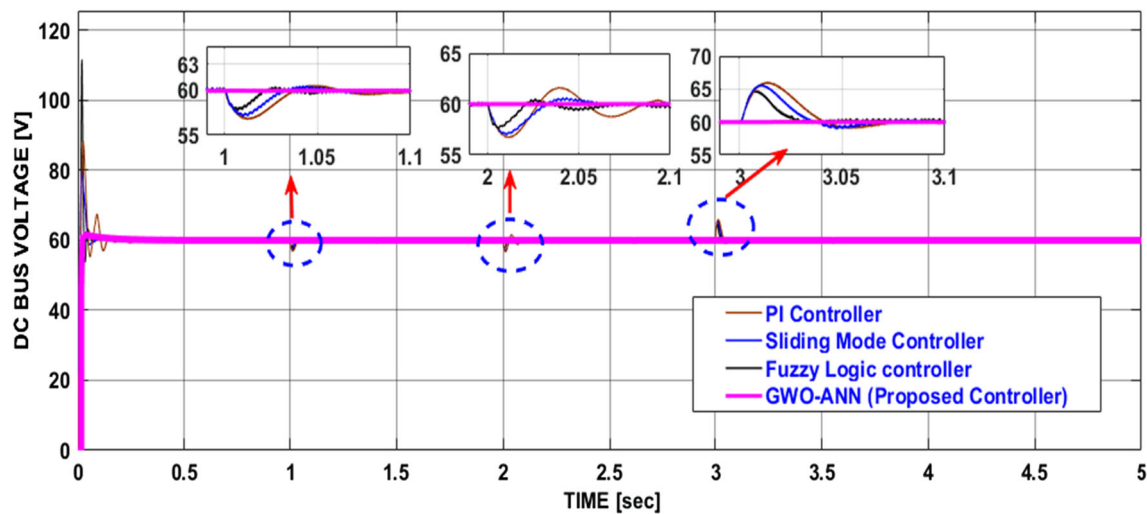
Fig. 17 The proposed method's DC link voltage was compared to that of conventional PI, sliding mode and FLC techniques

3.3 Dynamic performance of BESS controller

The primary task in this particular segment entails evaluating and scrutinizing the efficacy of the controller for the battery energy storage system (BESS). In order to achieve this, two different types of testing will be conducted. The first test involves sudden increases or decreases in power generation due to varying ecological conditions, while maintaining a constant load that is simulated over a period of 0 to 3 s. The second test involves constant power generation with variable load conditions that is simulated over a period of 3 to 4 s. The performance of the converter will then be compared with traditional control strategies. According to Fig. 17, the voltage of the bus experiences limited fluctuations due to the gradual changes in power generation.

The implementation of PI control results in a maximum fluctuation of $\Delta v = 5\%$. On the other hand, sliding mode control limits the maximum fluctuation to $\Delta v = 4.1\%$, while fuzzy logic control further improves the maximum fluctuation to $\Delta v = 2.5\%$. Ultimately, the proposed controller ensures that the voltage remains constant at 60 V. Simulation results indicate that the selected control strategy is capable of upholding the constancy of the DC bus voltage even in the presence of energy generation as well as load fluctuations. During fluctuations, the optimized ANN control method yields the best control effect, resulting in the bus voltage climbing to the rated value at 60 V. This is followed by sliding mode fuzzy logic and PI control. From the above observation, the least effective control strategy is found to be traditional PI controller.

3.4 Dynamic performance of hybrid renewable energy microgrid:

The hybrid renewable energy microgrid underwent three distinct case scenarios. The initial situation entailed the preservation of a consistent load state, while simultaneously altering the solar and wind energy inputs. In the subsequent situation, the demand for load was altered, while the renewable energy sources remained unchanged. The third scenario encompassed fluctuations in both the demand for energy and the availability of renewable energy resources. It is important to highlight that the simulation results were obtained in a consistent runtime of 5 s for both of these scenarios.

3.4.1 Varying generating conditions with consistent load

The primary objective of the initial case study is to ensure a consistent and uninterrupted power supply to the load by adapting to varying generating conditions. To achieve this, the level of irradiance was adjusted to 0 W/m^2, 400 W/m^2, 600 W/m^2 and 1000 W/m^2 during the time intervals of 0–1 s, 1–2 s, 2–3 s, and 3–5 s, respectively. Similarly, the wind speed underwent changes of 12 m/s, 10 m/s, 8 m/s, 9 m/s and 11 m/s during the time intervals of 0–0.5 s, 0.5–1 s, 1–2.5 s, 2.5–3.5 s and 3.5–5 s, respectively, as illustrated in Fig. 18a.

Based on Fig. 18, the intelligent energy management system utilized in small-scale microgrid operation is working effectively. The battery management system can keep a steady load power of 360 watts due to the variable power generation. During the initial stage, PV power is zero from 0–0.5 s, while wind power is at 100 W as shown in Fig. 18c. As a result, the battery storage will discharge and produce 260 W to compensate for the load demand. From 0.5 to 1 s, PV power remains at zero, and wind power is reduced
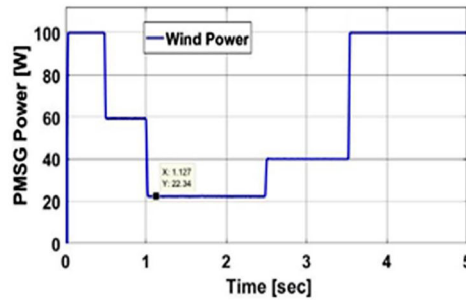
Fig. 18 The distribution of power across various points in the microgrid remains consistent despite the fluctuating supply of renewable energy sources
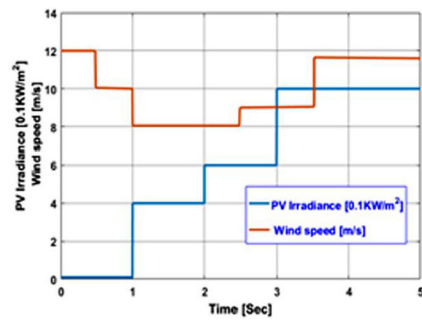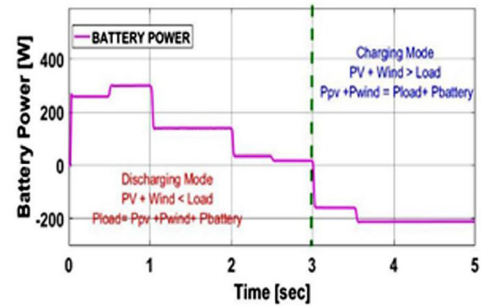

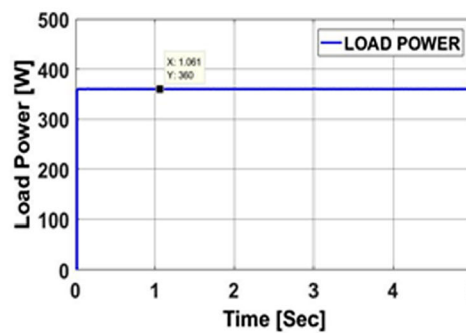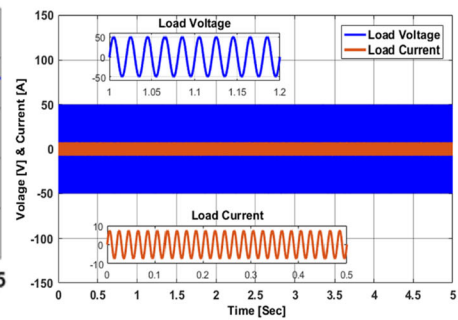a) **PV Irradiation & Wind Velocity**
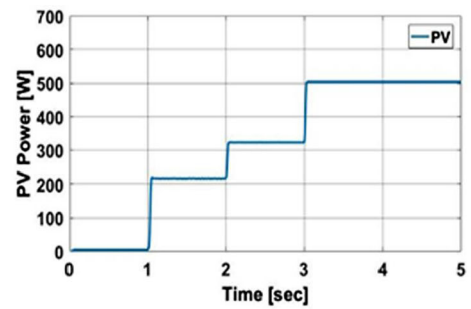
b) **PV Power**

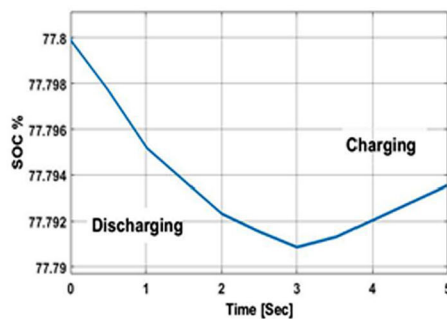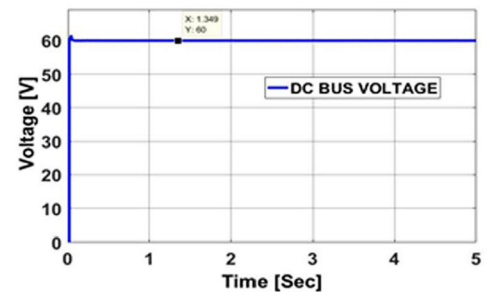c) **PMSG Power**

d) **Battery Power**

e) **Load Power**

f) **Load Voltage & Current**

g) **Battery SOC**

h) **DC Bus Voltage**

to 83 W. The battery produced 273W to maintain the load demand. From 1–2 s, the PV generates 210 W as shown in Fig. 18b, and wind power is reduced to 30W. The battery produced 120 W to maintain the load demand. From 2–3 s, PV power is at 320W, and wind power is at 40 W. The demand is satisfied by the hybrid system, and the battery will start charging mode after 3–5 s. The hybrid system maintains the load power while simultaneously charging from 0 to 2.5 s, the battery will discharge, and from 2.5 to 5 s, it will charge, as shown in Fig. 18d. Finally, the DC bus voltage maintains at 60 V, as depicted in Fig. 18h. The load voltage and current maintain a constant magnitude at different generations as shown in Fig. 18f.

3.4.2 Varying generating conditions with variable load

In this scenario, as previously mentioned, the ecological data for PV and WIND are identical, but the load power varies between 360 and 800W for different durations ranging from 0 to 5 s. The hybrid energy resource and battery storage system are employed in order to fulfill the fluctuating load requirements. Throughout the analysis, the battery discharging mode is activated for 0 to 5 s, ensuring that the DC bus voltage maintains at 60 V, as illustrated in Fig. 19a–h. Despite the different power generation levels, the load voltage remains consistent.

3.4.3 Real-world generation capabilities in a single day with a consistent load.

In this particular situation, we make use of 1-day worth of real-world ecological data for PV and WIND, along with a constant load that spans from 0 to 23 h. In order to address the variability in electricity production and fulfill the requirements of power consumption, we employ a hybrid energy resource and battery management system. Throughout the analysis, the battery discharging mode is turned on between 0 and 6 and 17 and 23 h, with the charging mode turned on between 6 and 17 h, while upholding a constant DC bus voltage of 60 V, as illustrated in Fig. 20a–d. Despite varying power generation levels, the load voltage remains consistently stable.

After conducting the aforementioned simulation work and analyzing the results, we have reached the conclusion that the suggested controller algorithm and intelligent energy management system function effectively under various ecological and load conditions, successfully maintaining the energy balance. The proposed controller algorithm demonstrates remarkable performance in rapidly changing conditions. In comparison to traditional controllers, our suggested controller is suitable for real-time environmental applications (Table 8).

4 Experimental validation and results

The experimental implementation of small-scale prototype modes for renewable energy based microgrid has been executed through the utilization of a DSPIC30F4011 controller board, as depicted in Fig. 21. The DSPIC30F4011 board is an adaptable and highly capable solution for low power microgrid applications, with features including power management, communication, digital signal processing, real-time control and energy management. This alternative is an exceptional pick for guaranteeing the steadiness, dependability and efficiency of microgrids, which perform an essential part in current power systems. As microgrids become increasingly important, the DSPIC30F4011 remains a reliable and versatile tool for effective management and control. The inclusion of IoT technology to supervise and regulate the system enhances its potential by enabling remote supervision, data-based decision-making and enhanced efficacy. This comprehensive method signifies a progressive remedy for generating and distributing sustainable and dependable energy in microgrid settings.

The DSPIC30F4011 comes preloaded with common control functions, eliminating the need for custom code compilation. Additionally, the controller can directly compile programs from C-code using the Simulink Real-Time Workshop library. The DSPIC30F4011 not only provides PWM and serial peripheral interface functionalities, but it also expertly manages the encoder interface and A/D modules. Consequently, the DSPIC30F4011 board proves to be an exceptional real-time controller that is perfectly suited for closed loop control applications.

The proposed hardware setup is made up of a PMSG coupled with a 0.5 HP induction motor, which can achieve varying wind speeds, while a PV emulator is used to adjust irradiation and temperature levels of PV input power. To store energy, a 12 V, 24 Ah lead acid battery is employed, and the suitable power converters for the PV, wind, battery and load are chosen. All the necessary components for the task at hand encompass encoders, line filter inductors, modules capable of handling variable loads with minimal power consumption, interfaces for seamless connectivity and devices for measuring voltage and current. Furthermore, NodalMCU is used for wireless communication to access data and control from all over the world. Table 9 provides a list of hardware equipment parameters. The microgrid system utilizes two DSPIC30F4011 controllers, with one of them functioning as the master controller and the other as the slave controller, as illustrated in Fig. 22. The slave controller is responsible for controlling the PV and wind energy conversion unit, while the master controller manages the BMS and inverter for load and grid control. The proposed controller that has been suggested is accountable for the acquisition of voltage
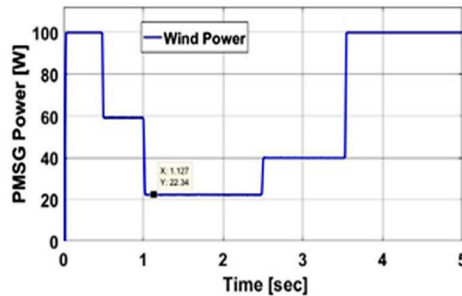
Fig. 19 The distribution of power in various sections of the microgrid changes depending on the fluctuating demand and the varying sources of renewable energy
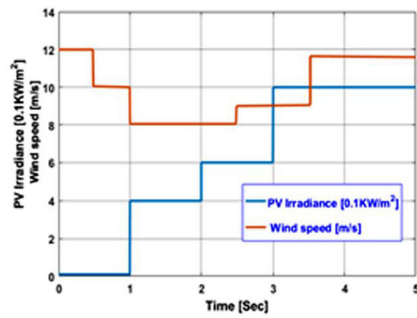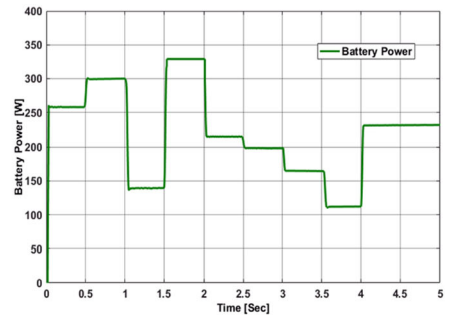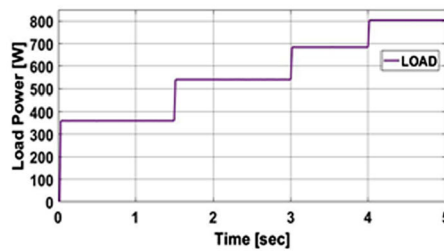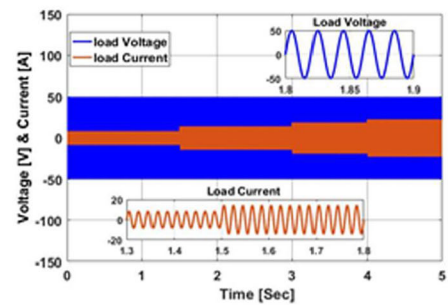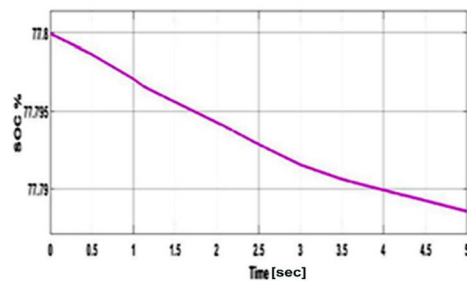
a) **PV Irradiation & Wind Velocity**
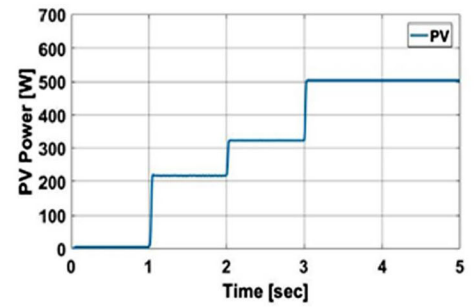
b) **PV Power**

c) **PMSG Power**

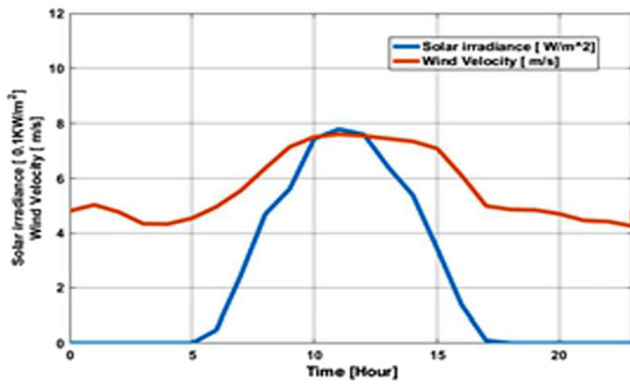d) **Battery Power**

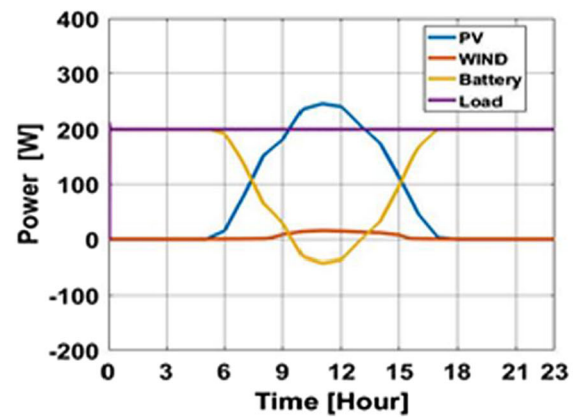e) **Load Power**
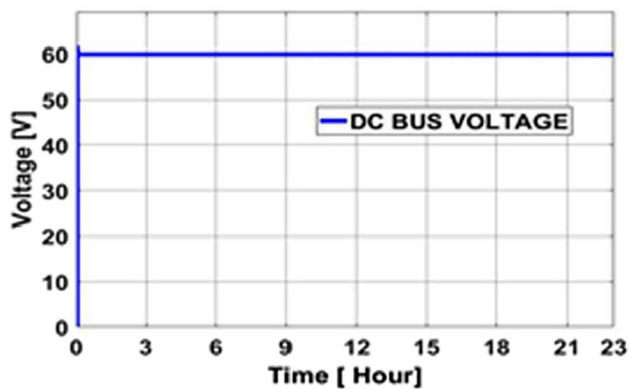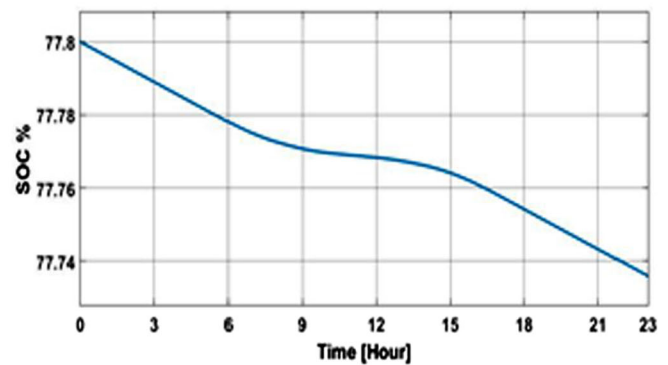
f) **Load Voltage & Current**
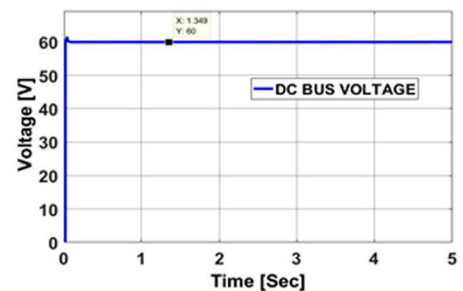
g) **Battery SOC**

h) **DC Bus Voltage**

a) **Solar Irradiation & Wind Velocity**

b) **Power for PV, wind, load & battery**

c) **DC Bus Voltage**

d) **Battery SOC**

Fig. 20 The distribution of power across various points in the microgrid remains consistent despite the fluctuating supply of renewable energy sources for one day

and current measurements from the power generation unit, energy storage unit and load unit.

The aforementioned measurements are subsequently conveyed to the intelligent energy management system and control algorithms for the purpose of determining the power levels at various points within the microgrid. Additionally, it evaluates the necessary measures to regulate the energy equilibrium within the system, producing the requisite pulse width modulations for the microgrid converters.

The assimilation of IoT technology grants the ability to remotely oversee and regulate the microgrid system. By employing sensors and NODEMCU ESP8266 communication module, the microgrid's data can be sent to a centralized control center or cloud-based platform. This remote access avails real-time performance monitoring, fault detection and the capability to adjust system parameters from afar. Moreover, it facilitates data analytics and anticipatory maintenance, thereby enhancing the overall effectiveness and dependability of the microgrid.

4.1 Experimental results

In this particular section of the research, the examination of empirical findings was carried out employing two distinct modalities: grid-connected and islanded mode in relation to the suggested small-scale microgrid system. The grid-connected operational mode was utilized to validate the correspondence between the inverter's voltage and frequency and those of the grid, as demonstrated in Fig. 23. Then, the suggested control system for the hybrid renewable energy based microgrid small-scale system, which combines photovoltaic (PV) and wind power, along with battery storage, was proven using the islanded mode. Numerous experimental scenarios were analyzed, encompassing various parameters including wind turbine velocity, solar irradiation, fluctuating load and situations involving low power output. This study involved examining three scenarios to assess the dependability of the system. The first scenario focused on a constant load with consistent PV and wind power, whereas the second scenario placed its focus on the inconsistent nature of
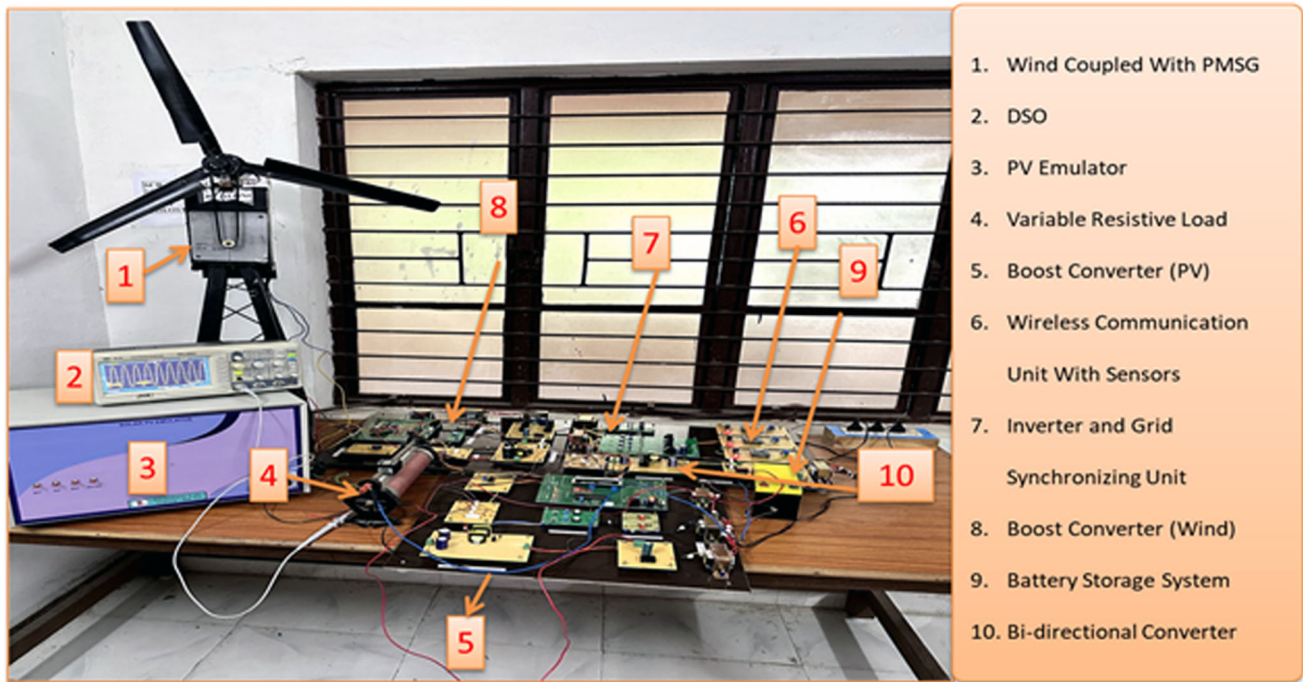
Fig. 21 Prototyping a small-scale hybrid solar–wind microgrid system

Table 9 Parameters of hardware equipment

| Conversion unit	Apparatus	Type	Rating
WECS	PMSG	Power, voltage, current	150 W, 18 V, 8.3 A
		Rated Speed	6000 RPM
	Boost converter	Inductance, capacitance	1mH, 100μF
	Voltage sensor	Voltage divider used	
	Current sensor	ACS712, current rating	0–30 A
	Wireless sensor	NODEMCU ESP8266	
SECS	PV emulator	Nominal Power	500 W, 12 V, 40 A
	Boost converter	Inductance, capacitance	1 mH, 100 μF
	Voltage sensor	Voltage divider used	
	Current sensor	ACS712, current rating	0–30 A
	Wireless sensor	NODEMCU ESP8266	
BESS	Battery	Voltage & Capacity	12 V & 24 Ah
	Boost converter	Inductance, capacitance	1 mH, 100 μF
	Voltage sensor	Voltage divider used	
	Current sensor	ACS712, current rating	0–30 A
	Wireless sensor	NODEMCU ESP8266	
	DC Bus	DC bus voltage reference, VDC	60 V
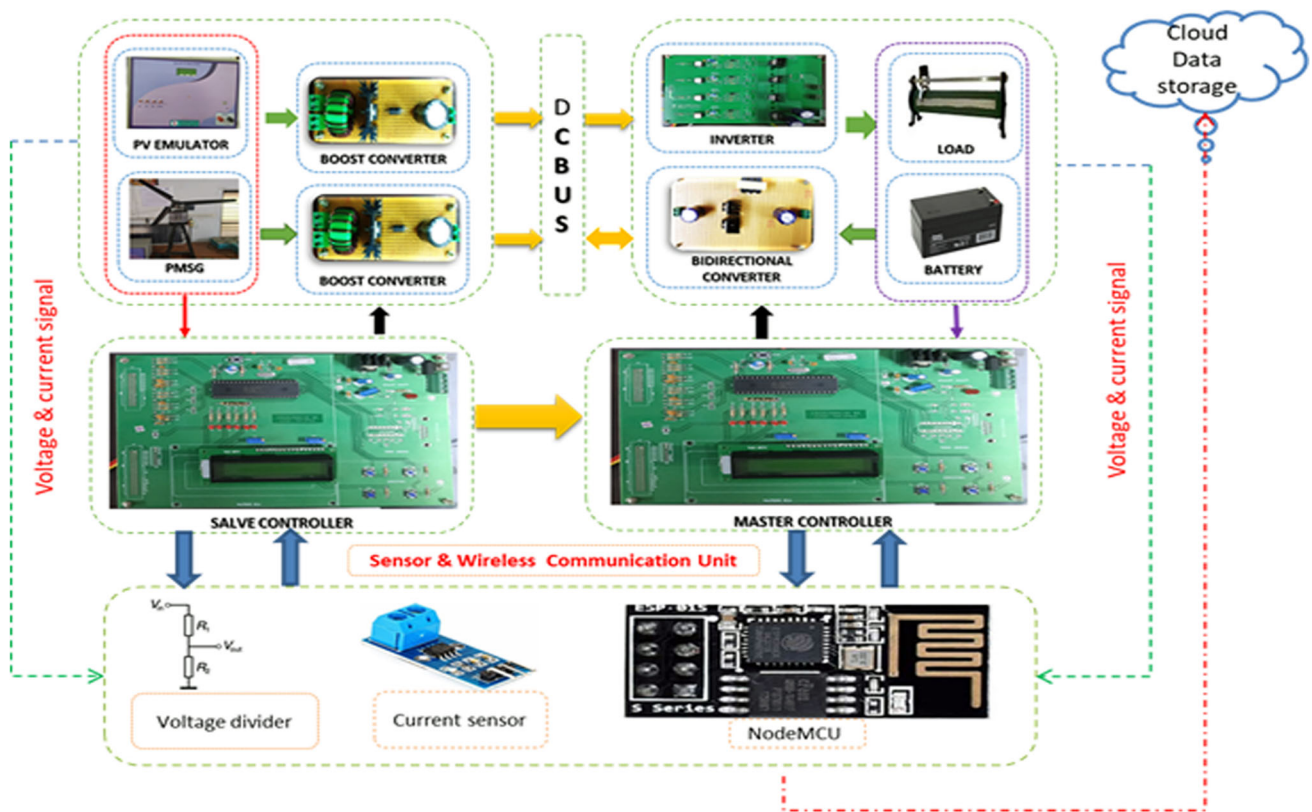
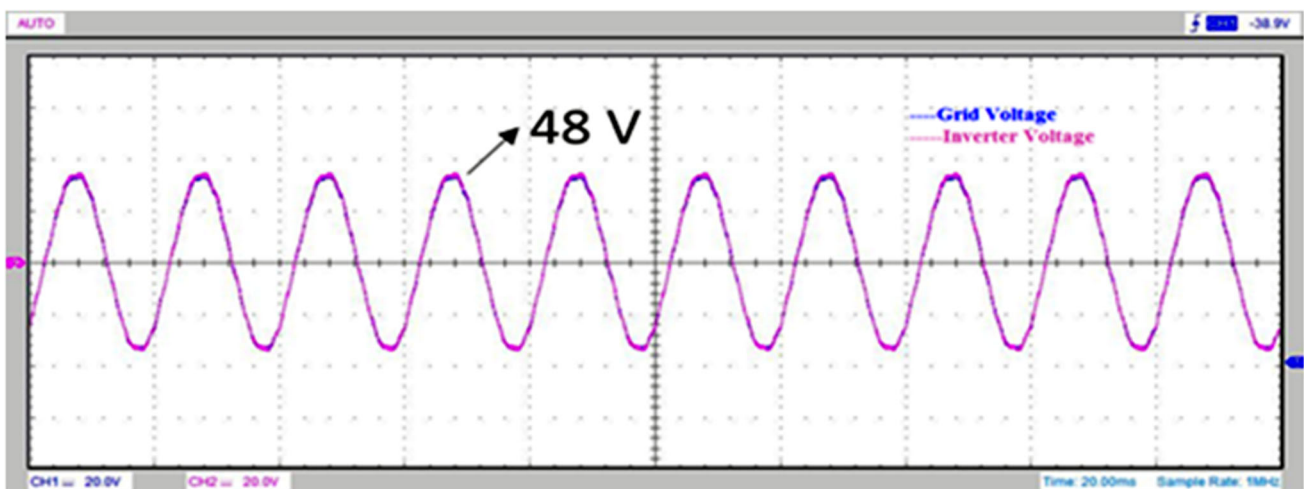Fig. 22 Schematic diagram of controller functions

Fig. 23 Hardware grid and inverter voltage

wind power and solar power, which can be unpredictable, while concurrently maintaining a constant load.

It is essential for the system to stay stable and guarantee a trustworthy energy output in such circumstances. The third scenario dealt with a constant renewable power generation and variable load, requiring battery power to supplement insufficient power generation from renewable sources. By analyzing these three scenarios, the hybrid power

system's reliability was established. In the fascinating realm of islanded mode operation, the rapid fluctuations in output can be visually observed through the use of a digital storage oscilloscope (DSO). However, this marvelous device only displays the instantaneous output. To capture and preserve the swift variations in output, we rely on the assistance of storage devices within the DSO. These invaluable storage devices allow us to store the rapid variation output, which

can then be conveniently exported to a CSV file. Once in this digital format, we can further analyze and visualize the results using the magnificent MATLAB software.

4.1.1 System performance under constant power generation and constant load

The prime objective of the initial scenario is to ensure a consistent amount of power to the load under stable power generation circumstances. In this particular case, a load of 200 watts was subjected to testing in an isolated microgrid mode. The load was powered by 100 watts from solar energy and 100 watts from wind energy. To achieve islanded mode, the inverter voltage was set to 48 V. The entire performance of both the power generation and load signals was visually observed using a digital signal oscilloscope, as depicted in Fig. 24.

4.1.2 The constant load can be balanced with diverse renewable energy sources.

The main focus of the second scenario is to guarantee a steady provision of electricity to the load despite fluctuating circumstances of power generation. In order to achieve this, the solar irradiance is adjusted utilizing a PV emulator, while the wind speed is adjusted through the use of a wind emulator. The solar irradiance varies at different time intervals, starting from the beginning and continuing at 0–1 min, 1–2 min, 2–3 min, 3–4 min and 4–5 min, with corresponding measurements of 500 W/m^2, 450 W/m^2, 300 W/m^2, 150 W/m^2 and 100 W/m^2 respectively. Similarly, the wind velocity is varied at the initial time and at time intervals of 0–0.5 min, 0.5–1.5 min, 1.5–2.5 min, 2.5–3.5 min and 3.5–5 min with corresponding values of 12 m/s, 11 m/s, 10 m/s and 9 m/s respectively, as depicted in Fig. 25a. It is essential to mention that these variations are only step variations and do not precisely represent the ever-changing real-world meteorological conditions. However, these values have been carefully selected to encompass the complete range of operation for the PV and wind energy conversion system, this deliberate selection allows for a comprehensive assessment of the performance of the system under varying conditions. Furthermore, it is important to note that the load, as depicted in Fig. 25e, remains constant at 100 W in this specific case. It should be acknowledged that in real-world scenarios, the load would not remain consistently fixed. The rationale behind maintaining a fixed load is to observe the performance of the renewable energy conversion systems and the battery storage system within a small-scale microgrid system. During the initial phase, PV power is at 160 W from 0–1 min, while wind power is at 100 W as illustrated in Fig. 25b, d. Consequently, the battery storage will charge to compensate for the load demand in the hybrid system. Between 1–2 min,

PV power decreases to 140 W, and wind power decreases to 70 W. This leads to the battery storage charging to meet the load demand. Moving on to 2–3 min, PV generates 100 W as seen in Fig. 25b, and wind power drops to 60 W. This results in the battery storage charging to address the load demand. From 3.5 to 4 min, PV power is 50 W, and wind power is 40 W. Consequently, the battery storage discharges and produces 10 W to meet the load demand. Between 4–5 min, PV power is 40 W, and wind power is 70 W. This causes the battery storage to charge to compensate for the load demand. The consistent load can be managed by various renewable energy sources from 0 to 3 min as the battery charges, from 3 to 3.5 min a lag in generation occurs, leading to the battery balancing the demand and initiating a discharging operation. The remaining interval sees the battery charging. According to the research findings, energy wastage is minimized, and power supply reliability is maintained with the assistance of EMS. Ultimately, the DC bus voltage remains stable at 60 V, as shown in Fig. 25h. The load voltage and current maintain a constant magnitude during different generation stages as depicted in Fig. 25f, g.

### 4.1.3 Constant renewable power generation and variable load

In the alternate scenario, the continuous production of solar and wind power remains unaltered, with solar power of 100 W in irradiance remaining steadfast at 300W/m^2 and wind power at 55 W in 10 m/s wind velocity, as illustrated in Fig. 26a. At intervals of 1 min, the energy demand fluctuates, thus subjecting the effectiveness of the microgrid to the challenge of varying energy requirements. At the outset, the load requirement is established at 100 W, wherein 100 W of energy is obtained from renewable sources, and the residual 55 W of energy is accumulated in a battery storage apparatus. From 1 to 5 min, the demand escalates rapidly, enabling the surplus power generated during this period to recharge the battery. Subsequently, after 1 min, the demand surpasses the supply, leading to the battery supplying the additional power required, as depicted in Fig. 26d. Throughout these fluctuations in load, the microgrid consistently maintains a steady voltage at the load terminal, as demonstrated in Fig. 26e. The EMS successfully maintains equilibrium of power when faced with varying load demands, encompassing both lower and higher levels. Meanwhile, the power generated from sustainable energy sources remains steady. The battery charges when the load demand decreases, but releases its stored energy when the load demand increases.

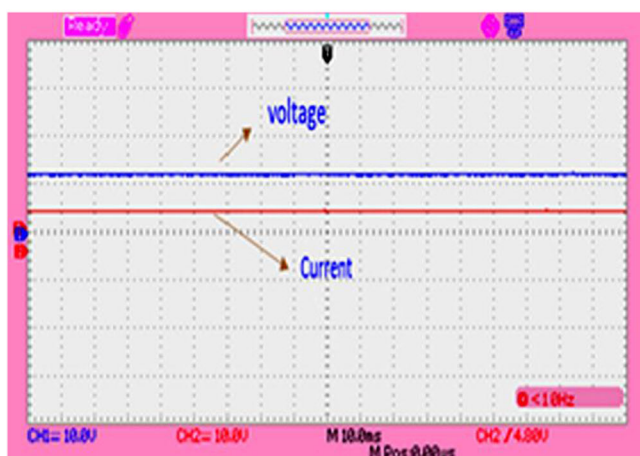### 4.1.4 Data monitoring system output (IoT)

The incorporation of NodeMCU ESP8266-based monitoring devices in a small-scale microgrid system offers an affordable
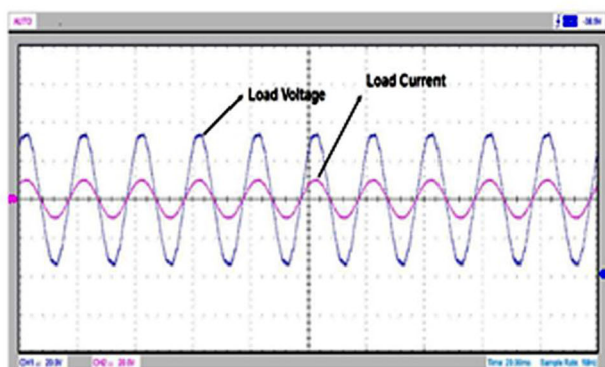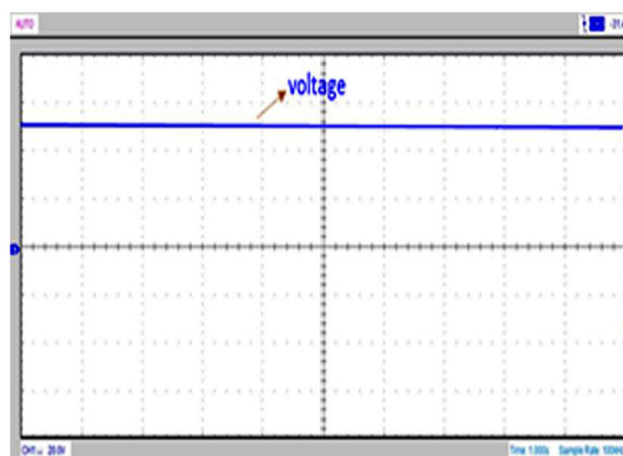
(a) Load Voltage & Current
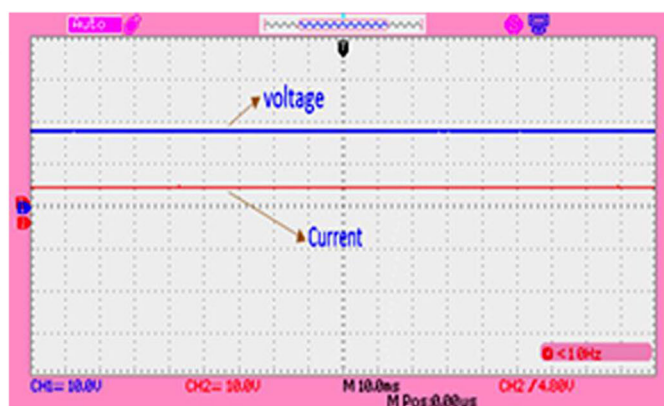
(b) Wind Voltage & Current

(c) PV Voltage & Current

(d) DC Bus Voltage

Fig. 24 Hardware output—constant generation power and constant load

and efficient solution for monitoring different parameters of solar, wind and battery storage systems. By accessing data online through the Adafruit platform, users are able to conveniently monitor renewable energy systems from any location around the globe, thus facilitating efficient energy management and optimization. The specific methodology mentioned plays a substantial part in advancing the acceptance of sustainable energy sources through the improvement of the reach and feasibility of tracking capabilities. Figure 27 showcases data that are visually displayed on an online website, illustrating constant power generation and load condition scenarios in a case study.

5 Conclusion

In this research work, we successfully designed and developed an intelligent energy management system (EMS) tailored for a small-scale microgrid, catering to remote communities. Here, three major tasks such as designing a GWO-tuned ANN controller for hybrid system, IoT-based monitoring and intelligent energy management for small-scale microgrid system are successfully achieved. In the initial stages of designing an artificial neural network (ANN) controller, it is imperative to first acquire significant data. This involves the collection of real data over a period of 210 days, equivalent to 5040 h, through the NASA Research Center. The utilization of significant data is crucial in preventing overfitting and mitigating the rapid fluctuations in input variables, thereby ensuring the generation of accurate outputs by the controller through the training on such data. Subsequently, the significant parameters of ANN such as initial weight and hidden layer are optimized by grey wolf optimizer during the computation process. The results revealed notable improvements in mean-squared error (MSE) values
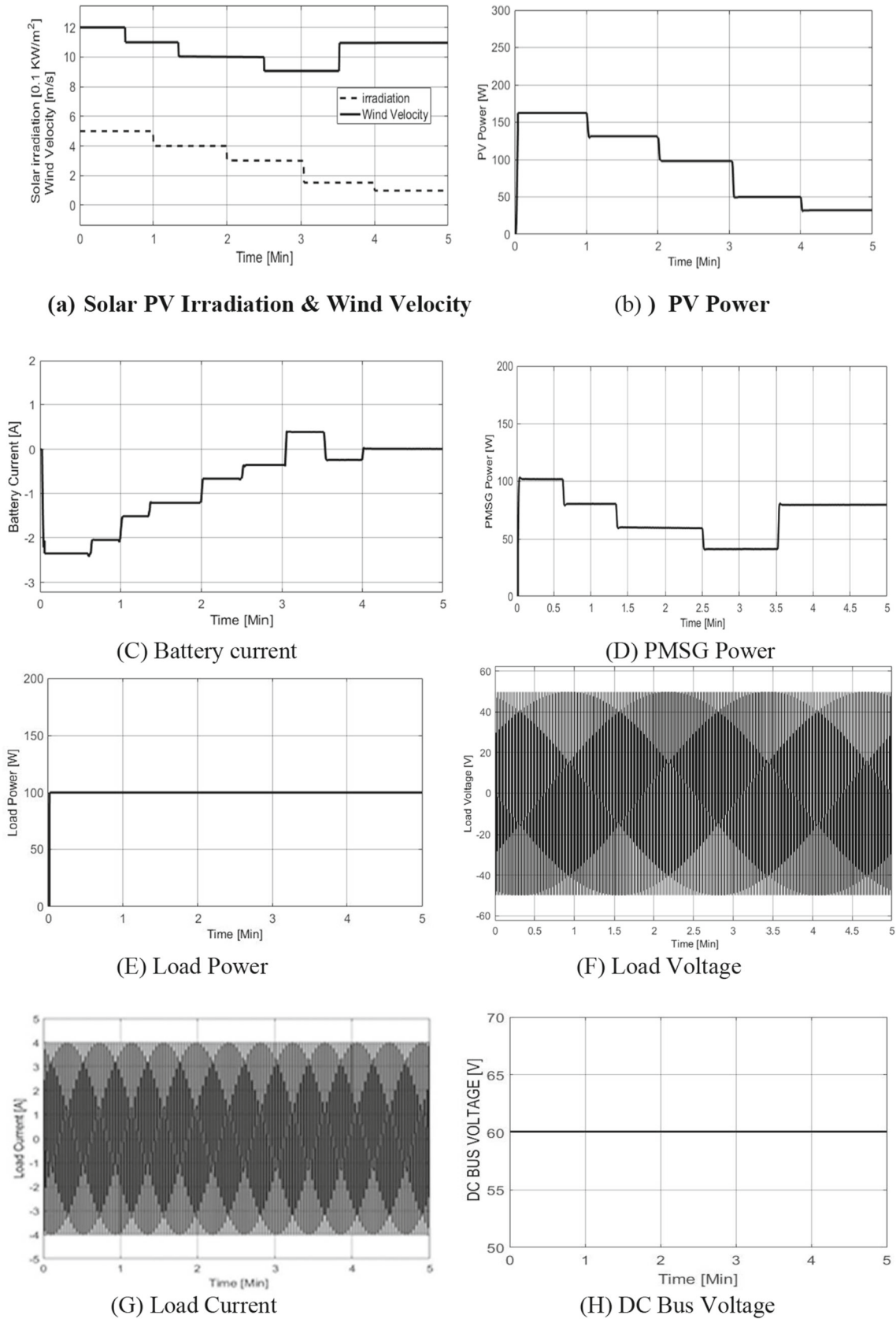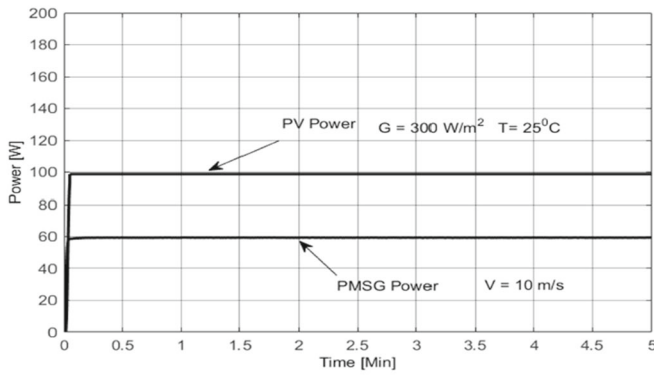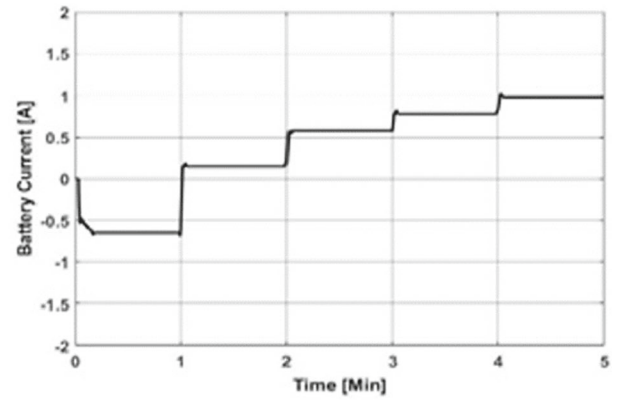
(a) Solar PV Irradiation & Wind Velocity

(b)) PV Power

(C) Battery current

(D) PMSG Power

(E) Load Power

(F) Load Voltage

(G) Load Current
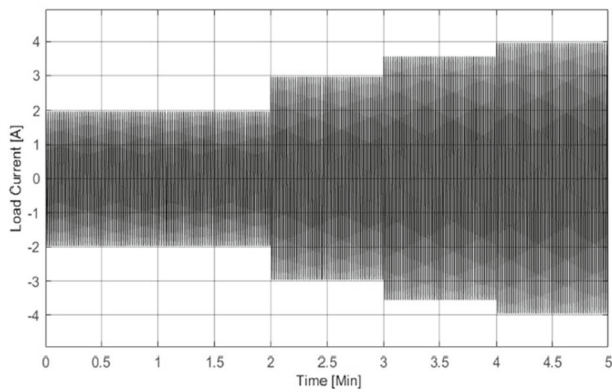
(H) DC Bus Voltage

Fig. 25 The distribution of power in various sections of the microgrid changes depending on the constant demand and the varying sources of renewable energy
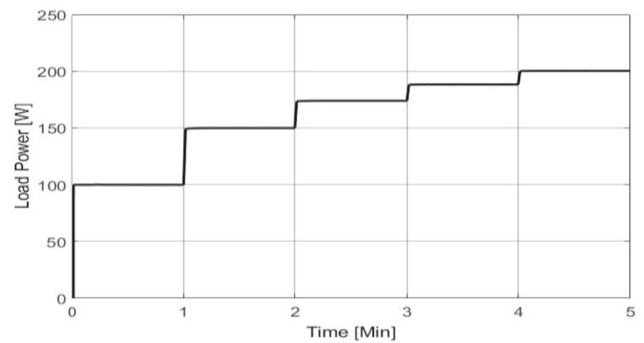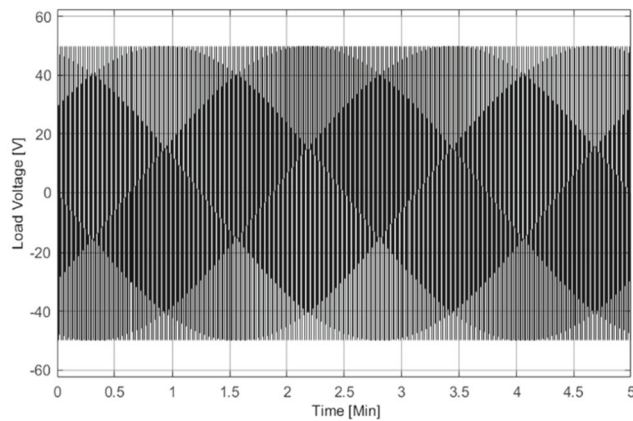
(a) PV & PMSG Power

(b) Battery Current
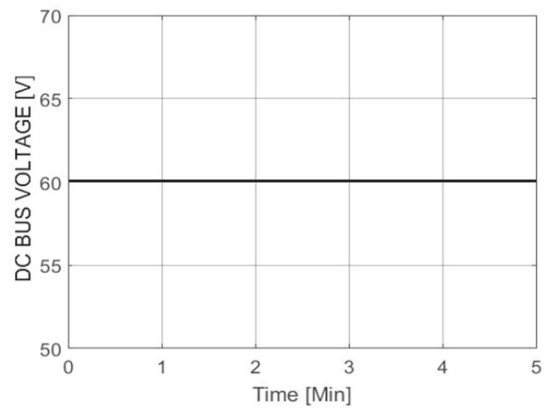

(c) Load current

(d) Load Power

(e) Load Voltage

(f) DC Bus Voltage

Fig. 26 The distribution of power in various sections of the microgrid changes depending on the fluctuating demand and the constant sources of renewable energy
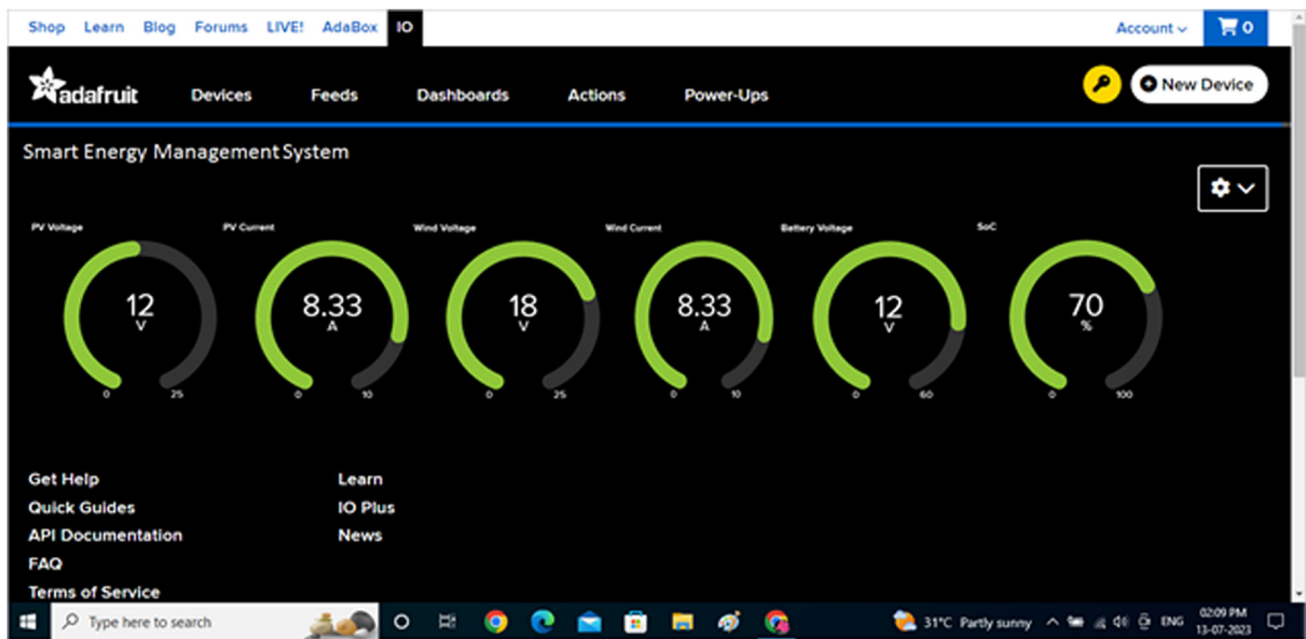
Fig. 27 Proposed system communication data visually displayed on an online website

when compared to the conventional back-propagation technique. Specifically, the MSE values were 0.00978, 0.0500 and 0.0440 for the solar, wind and battery controllers, respectively, under the conventional method, whereas they were 0.0040, 0.0065 and 0.0022 under the GWO-tuned approach. Due to minimization of MSE, the tracking ability of the controller is improved and extracted the maximum power as system output. Simultaneously, the performance the battery storage system is improved. Even though rapid variation of demand as well as generation, the DC bus voltage is maintained consistently. For simulation process, considering the proposed system is required to meet 200 watts as load demand in islanded mode. Here, PV produced 100 watts for 300 m/s^2 as solar irritation and wind produced 55 watts for 10 m/s as wind velocity. Hence, total power is produced in this system is around 155 watts which is insufficient to meet the demand. In this instant, based on the response of IoT and smart EMS, instruction has been given to the controller which initiates the battery storage unit to provide rest of the power (45 watts) to meet the load demand. Same environment has been applied for experimental validation of proposed system which has produced same output as obtained in simulation result. In future, this system will help to analyze fault identification, integration of distributed energy resources like biomass, mini hydropower generation and reduction of GHG emission.

Author contributions All authors are contributed equally to this work.

Data availability No datasets were generated or analyzed during the current study.

Declarations

Conflict of interest The authors declare no competing interests.

References

1. Dogan E, Seker F (2016) The influence of real output, renewable and non-renewable energy, trade and financial development on carbon emissions in the top renewable energy countries. 60. https://doi.org/10.1016/J.RSER.2016.02.006
2. Brenna M, Longo M, Yaïci W, Abegaz TD (2017) Simulation and optimization of integration of hybrid renewable energy sources and storages for remote communities electrification. https://doi.org/10.1109/isgteurope.2017.8260274
3. Halabi LM, Mekhilef S (2018) Flexible hybrid renewable energy system design for a typical remote village located in tropical climate. J Clean Prod 177:908–924. https://doi.org/10.1016/j.jclepro.2017.12.248
4. Yaakub MF, Noh FHM, Zali MFIM, Harun M (2020) Prospective study of power generation from natural resources using hybrid system for remote area. Indones J Electr Eng Comput Sci. https://doi.org/10.11591/ijeecs.v18.i2.pp642-647
5. You V, Kakinaka M (2021) Modern and traditional renewable energy sources and CO2 emissions in emerging countries. Environ Sci Pollut Res 29(12):17695–17708. https://doi.org/10.1007/s11356-021-16669-2
6. Abdel-Gawad H, Sood VK (2019) A comprehensive review on microgrid architectures for distributed generation. https://doi.org/10.1109/epec47565.2019.9074800
7. Cagnano A, De Tuglie EE, Mancarella P (2020) Microgrids: overview and guidelines for practical implementations and operation. Appl Energy 258:114039. https://doi.org/10.1016/j.apenergy.2019.114039
8. Correa CM, Marulanda GA, Garces A (2016) Optimal microgrid management in the Colombian energy market with demand

response and energy storage. https://doi.org/10.1109/pesgm. 2016.7741905

9. Hirsch A, Parag Y, Guerrero JM (2018) Microgrids: a review of technologies, key drivers, and outstanding issues. Renew Sustain Energy Rev 90:402–411. https://doi.org/10.1016/j.rser.2018. 03.040

10. Milczarek A, Malinowski M, Guerrero JM (2015) Reactive power management in islanded microgrid—proportional power sharing in hierarchical droop control. IEEE Trans Smart Grid 6(4):1631–1638. https://doi.org/10.1109/tsg.2015.2396639

11. Rezkallah M, Chandra A, Singh B, Singh SK (2019) Microgrid: configurations, control and applications. IEEE Trans Smart Grid 10(2):1290–1302. https://doi.org/10.1109/tsg.2017.2762349

12. Balasingam B, Ahmed M, Pattipati KR (2020) Battery management systems—challenges and some solutions. Energies 13(11):2825. https://doi.org/10.3390/en13112825

13. Jossen A, Spath V, Döring H, Garche J (1999) Reliable battery operation—a challenge for the battery management system. J Power Sources 84(2):283–286. https://doi.org/10.1016/s0378-7753(99)00329-8

14. Lelie M, Braun T, Knips M, Nordmann H, Ringbeck F, Zappen H, Sauer DU (2018) Battery management system hardware concepts: an overview. Appl Sci 8(4):534. https://doi.org/10.3390/app8040534

15. Wang J, Yin Z (2021) Overview of key technologies of battery management system. J Phys 2030(1):012009. https://doi.org/10.1088/1742-6596/2030/1/012009

16. Alhasnawi B, Jasim B (2020) Adaptive energy management system for smart hybrid microgrids. Iraqi J Electr Electron Eng sceeer(3d):73–85. https://doi.org/10.37917/ijeee.sceeer.3rd.11

17. Carignano M, Roda V, Costa-Castelló R, Valiño L, Lozano A, Barreras F (2019) Assessment of energy management in a fuel cell/battery hybrid vehicle. IEEE Access 7:16110–16122. https://doi.org/10.1109/access.2018.2889738

18. Kamel A, Rezk H, Abdelkareem MA (2021) Enhancing the operation of fuel cell-photovoltaic-battery-supercapacitor renewable system through a hybrid energy management strategy. Int J Hydrogen Energy 46(8):6061–6075. https://doi.org/10.1016/j.ijhydene.2020.06.052

19. Marzougui H, Kadri A, Martin J, Amari M, Pierfederici S, Bacha F (2019) Implementation of energy management strategy of hybrid power source for electrical vehicle. Energy Convers Manag 195:830–843. https://doi.org/10.1016/j.enconman.2019.05.037

20. Rajagopal JK, Thangavel V (2020) Analysis of energy management in micro-grid with distributed generation system. Am J Modern Energy 6(6):117. https://doi.org/10.11648/j.ajme.20200606.12

21. Salah O, Shamayleh A, Mukhopadhyay S (2021) Energy management of a multi-source power system. Algorithms 14(7):206. https://doi.org/10.3390/a14070206

22. Yan N, Zhong Y, Li X, Wang Y, Su L, Jiang W, Zhou J (2021) Energy management method of electricity heat hydrogen multi-coupling system for retired power battery echelon utilization in microgrids. IEEE Trans Appl Supercond 31(8):1–5. https://doi.org/10.1109/tasc.2021.3110471

23. Al-Rawashdeh H, Al-Khashman OA, Bdour JTA, Gomaa MR, Rezk H, Marashli A, Arrfou LM, Louzazni M (2023) Performance analysis of a hybrid renewable-energy system for green buildings to improve efficiency and reduce GHG emissions with multiple scenarios. Sustainability 15(9):7529. https://doi.org/10.3390/su15097529

24. Bakht MP, Mohd MNH, Shahrin M, Ayob NK, Bukar AL (2023) A community scale hybrid renewable energy system for sustainable power supply during load shedding. Indones J Electr Eng Comput Sci 31(1):33. https://doi.org/10.11591/ijeecs.v31.i1.pp33-43

25. Hassan Q, Jaszczur M, Abdulrahman IS, Salman HM (2022) An economic and technological analysis of hybrid photovoltaic/wind turbine/battery renewable energy system with the highest self-sustainability. Energy Harvest Syst 10(2):247–257. https://doi.org/10.1515/ehs-2022-0030

26. Jha N, Prashar D, Rashid M, Khanam Z, Nagpal A, AlGhamdi AS, Alshamrani SS (2022) Energy-efficient hybrid power system model based on solar and wind energy for integrated grids. Math Probl Eng 2022:1–12. https://doi.org/10.1155/2022/4877422

27. Khorgade S, Wankhede A, Gajbhiye A, Ramteke A, Wath S, Sarpate Y (2023) Integrated power system using wind and solar energy. Int J Res Appl Sci Eng Technol 11(4):600–606. https://doi.org/10.22214/ijraset.2023.50154

28. Manusmare PV, Bonde UG, Bawane DA (2023) Modeling of hybrid renewable energy system. Int J Res Appl Sci Eng Technol 11(3):1226–1231. https://doi.org/10.22214/ijraset.2023.49639

29. Mishra A (2023) Analysis and implementation of a three-phase grid-connected PV/WIND hybrid system. Int J Res Appl Sci Eng Technol 11(6):1061–1076. https://doi.org/10.22214/ijraset.2023.53813

30. Reuchlin S, Joshi R, Schmehl R (2023) Sizing of hybrid power systems for Off-Grid applications using airborne wind energy. Energies 16(10):4036. https://doi.org/10.3390/en16104036

31. Rojas JP, García GR, Castillo DV (2022) Economic and environmental multiobjective optimization of a hybrid power generation system using solar and wind energy source. Int J Energy Econ Policy 12(1):494–499. https://doi.org/10.32479/ijeep.11864

32. Srivastava S (2022) Generation of hybrid energy system (Solar-Wind) supported with battery energy storage. Int J Res Appl Sci Eng Technol 10(9):1439–1446. https://doi.org/10.22214/ijraset.2022.46864

33. Gómez JC, De León-Aldaco SE, Aguayo J (2023) A review of hybrid renewable energy systems: architectures, battery systems, and optimization techniques. Eng 4(2):1446–1467. https://doi.org/10.3390/eng4020084

34. Sabir B, Lu S, Liu H, Lin C, Sarwar A, Huang L (2023) A novel isolated intelligent adjustable buck-boost converter with hill climbing MPPT algorithm for solar power systems. Processes 11(4):1010. https://doi.org/10.3390/pr11041010

35. Raj A, Arya SR, Gupta J (2020) Solar PV array-based DC–DC converter with MPPT for low power applications. Renew Energy Focus 34:109–119. https://doi.org/10.1016/j.ref.2020.05.003

36. Zakzouk NE, Elsaharty MA, Abdelsalam A, Helal AN, Williams BW (2016) Improved performance low-cost incremental conductance PV MPPT technique. IET Renew Power Gener 10(4):561–574. https://doi.org/10.1049/iet-rpg.2015.0203

37. Ali A, Li W, He X (2016) Performance analysis of incremental conductance MPPT with simple moving voltage average method for distributed PV system. Open Electr Electron Eng J 10(1):118–128. https://doi.org/10.2174/1874129001610010118

38. Owusu-Nyarko I, Elgenedy MA, Abdelsalam I, Ahmed K (2021) Modified variable step-size incremental conductance MPPT technique for photovoltaic systems. Electronics 10(19):2331. https://doi.org/10.3390/electronics10192331

39. Tian Y, Xia B, Xu Z, Sun W (2014) Modified asymmetrical variable step size incremental conductance maximum power point tracking method for photovoltaic systems. J Power Electron. https://doi.org/10.6113/jpe.2014.14.1.156

40. Reza MH, Shobug A (2020) Efficiency evaluation of P&O MPPT technique used for maximum power extraction from solar photovoltaic system. In: 2020 IEEE region 10 symposium (TENSYMP). https://doi.org/10.1109/tensymp50017.2020.9230810

41. Rezaei M, Asadi H (2019) A modified perturb-and-observe-based maximum power point tracking technique for photovoltaic energy conversion systems. J Control Autom Electr Syst 30(5):822–831. https://doi.org/10.1007/s40313-019-00495-6

42. Satapathy SS, Kumar N (2019) Modulated perturb and observe maximum power point tracking algorithm for solar PV energy conversion system. https://doi.org/10.1109/rdcape47089.2019.8979025

43. Huynh DC (2014) MPPT of solar PV panels using Chaos PSO algorithm under varying atmospheric conditions. Int J Eng Trends Technol 15(8):383–388. https://doi.org/10.14445/22315381/IJETT-V15P274

44. Kaced K, Larbes C, Ait-Chikh SM, Bounabi M, Dahmane ZE (2017) FPGA implementation of PSO based MPPT for PV systems under partial shading conditions. https://doi.org/10.1109/icosc.2017.7958682

45. Oliveira FR, Da Silva S, Durand FR, Sampaio LP (2015) Application of PSO method for maximum power point extraction in photovoltaic systems under partial shading conditions. https://doi.org/10.1109/cobep.2015.7420175

46. Syafaah L, Faruq A, NoorCahyadi B, Hidayat K, Setyawan N, Lestandy M, Zulfatman Z (2023) Design of MPPT for buck-boost converter based on GA to optimize solar power generation. Kinetik: Game Technol Inf Syst Comput Netw Comput Electron Control. https://doi.org/10.22219/kinetik.v8i3.1658

47. Mohanty S, Subudhi B, Ray PK (2016) A new MPPT design using grey wolf optimization technique for photovoltaic system under partial shading conditions. IEEE Trans Sustain Energy 7(1):181–188. https://doi.org/10.1109/tste.2015.2482120

48. Dhieb Y, Yaich MI, Bouzguenda M, Ghariani M (2022) MPPT optimization using ant colony algorithm: solar PV applications. In: 2022 IEEE 21st international conference on sciences and techniques of automatic control and computer engineering (STA). https://doi.org/10.1109/sta56120.2022.10019072

49. Development of rapid and reliable cuckoo search algorithm for global maximum power point tracking of solar PV systems in partial shading condition (2023) Archives of Control Sciences. https://doi.org/10.24425/acs.2021.138690

50. Satheesh Krishnan G, Kinattingal S, Simon SP, Nayak PSR (2020) MPPT in PV systems using ant colony optimisation with dwindling population. IET Renew Power Gener 14(7):1105–1112. https://doi.org/10.1049/iet-rpg.2019.0875

51. Chao K, Nguyen TQ (2024) Global maximum power point tracking of a photovoltaic module array based on modified CAT swarm optimization. Appl Sci (Basel) 14(7):2853. https://doi.org/10.3390/app14072853

52. A novel global maximum power point tracking method for PV system using Jaya algorithm. (2017) IEEE Conference Publication | IEEE Xplore. https://doi.org/10.1109/EI2.2017.8245345

53. Watanabe RB, Ando OH, Leandro PGM, Salvadori F, Beck MF, Pereira K, Brandt MHM, De Oliveira FM (2022) Implementation of the bio-inspired Metaheuristic Firefly Algorithm (FA) applied to maximum power point tracking of photovoltaic systems. Energies 15(15):5338. https://doi.org/10.3390/en15155338

54. Ebrahim EA (2016) Bacteria-foraging based-control of high-performance railway level-crossing safety drives fed from photovoltaic array. J Electr Syst Inf Technol 3(3):485–512. https://doi.org/10.1016/j.jesit.2015.11.014

55. Tagayi RK, Baek J, Kim J (2023) Flower pollination global peak search algorithm for partially shaded solar photovoltaic system. J Build Eng 66:105818. https://doi.org/10.1016/j.jobe.2022.105818

56. Pervez I, Sarwar A, Tayyab M, Sarfraz M (2019b) Gravitational search algorithm (GSA) based maximum power point tracking in a solar pv based generation system. In: 2019 Innovations in power and advanced computing technologies (i-PACT). https://doi.org/10.1109/i-pact44901.2019.8960130.

57. Alshareef M (2021) An improved MPPT method based on fuzzy logic controller for a PV system. Stud Inf Control 30(1):89–98. https://doi.org/10.24846/v30i1y202108

58. Chen Y, Jhang Y, Liang R (2016) A fuzzy-logic based auto-scaling variable step-size MPPT method for PV systems. Sol Energy 126:53–63. https://doi.org/10.1016/j.solener.2016.01.007

59. Ganthia BP, Pradhan R, Das S, Ganthia S (2017) Analytical study of MPPT based PV system using fuzzy logic controller. https://doi.org/10.1109/icecds.2017.8390063

60. Lazizi A, Kesraoui M, Chaib A (2016) Fuzzy logic MPPT control for a solar PV module applied to water pumping. Int J Ind Electron Drives 3(1):1. https://doi.org/10.1504/ijied.2016.077676

61. Samosir AS, Gusmedi H, Purwiyanti S, Komalasari E (2018) Modeling and simulation of fuzzy logic based maximum power point tracking (MPPT) for PV application. Int J Electr Comput Eng 8(3):1315. https://doi.org/10.11591/ijece.v8i3.pp1315-1323

62. Bouselham L, Hajji M, Hajji B, Bouali H (2016) A MPPT-based ANN controller applied to PV pumping system. https://doi.org/10.1109/irsec.2016.7983918

63. Djalab A, Sabri N, Teta A (2020) Maximum power point tracking (MPPT) for a PV system based on artificial neural network ANN and comparison with P&O algorithm. Lecture notes in electrical engineering. Springer Science+Business Media

64. Kumar A, Saha PK, Shekhar S (2019) Cascaded artificial neural network based MPPT algorithm for PV application. https://doi.org/10.1109/iceca.2019.8821949

65. Rizzo SA, Scelba G (2015) ANN based MPPT method for rapidly variable shading conditions. Appl Energy 145:124–132. https://doi.org/10.1016/j.apenergy.2015.01.077

66. Saeed F, Yousuf MA, Tauqeer HA, Akhtar M, Abbas Z, Khan MS (2021) Performance benchmark of multi-layer neural network based solar MPPT for PV applications. https://doi.org/10.1109/icept51706.2021.9435583

67. Shi Y, Li S, Wang S, Zhai Y, Tian Y, Yu D (2021) Pitch angle control with fault diagnosis and tolerance for wind turbine generation systems. Proc Inst Mech Eng Part I J Syst Control Eng 235(8):1355–1366. https://doi.org/10.1177/0959651821993689

68. Yurdusev MA, Ata R, Çetin NS (2006) Assessment of optimum tip speed ratio in wind turbines using artificial neural networks. Energy (Oxford) 31(12):2153–2161. https://doi.org/10.1016/j.energy.2005.09.007

69. Yuhendri M, Muskhir M, Taali T (2019) A novel optimum tip speed ratio control of low speed wind turbine generator based on type-2 fuzzy system. Bull Electr Eng Inform. https://doi.org/10.11591/eei.v8i4.1450

70. Hannachi M, Elbeji O, Benhamed M, Sbita L (2020) Optimal torque maximum power point technique for wind turbine: proportional–integral controller tuning based on particle swarm optimization. Wind Eng 45(2):337–350. https://doi.org/10.1177/0309524x19892903

71. Mousa HHH, Youssef A, Mohamed EEM (2021) State of the art perturb and observe MPPT algorithms based wind energy conversion systems: a technology review. Int J Electr Power Energy Syst 126:106598. https://doi.org/10.1016/j.ijepes.2020.106598

72. Kumari S, Bhakar PS, Gupta TN (2018) Analysis of Wind fed PMSG with INC MPPT using Interleaved Boost Converter. In: 2018 International conference on power energy, environment and intelligent control (PEEIC). https://doi.org/10.1109/peeic.2018.8665628

73. Mansouri M, Bey M, Hassaine S, Larbi M, Allaoui T, Denaï M (2022) Genetic algorithm optimized robust nonlinear observer for a wind turbine system based on permanent magnet synchronous generator. ISA Trans 129:230–242. https://doi.org/10.1016/j.isatra.2022.02.004

74. Chetouani E, Errami Y, Obbadi A, Sahnoun S (2021) Maximum power point tracking design using particle swarm optimization algorithm for wind energy conversion system connected to the grid. Renewable Energy Systems. Elsevier, pp 445–470. https://doi.org/10.1016/B978-0-12-820004-9.00009-7

75. Kumar CC, Raglend IJ (2018) A MPPT strategy based on cuckoo search for wind energy conversion system. Int J Eng Technol 7(4):2298. https://doi.org/10.14419/ijet.v7i4.17366

76. Rashmi G, Linda MM (2023) A novel MPPT design for a wind energy conversion system using grey wolf optimization. Automatika (Zagreb) 64(4):798–806. https://doi.org/10.1080/00051144.2023.2218168

77. Aruna R, Balaraman S (2021) Fuzzy Logic control based maximum power point tracking for wind energy conversion system. Int J Adv Res Sci Commun Technol. https://doi.org/10.48175/IJARSCT-1475

78. Tiwari R, Krishnamurthy K, Neelakandan RB, Padmanaban S, Wheeler P (2018) Neural network based maximum power point tracking control with quadratic boost converter for PMSG—wind energy conversion system. Electronics 7(2):20. https://doi.org/10.3390/electronics7020020

79. PWM based Double loop PI Control of a Bidirectional DC-DC Converter in a Standalone PV/Battery DC Power System (2019) IEEE Conference Publication | IEEE Xplore. https://ieeexplore.ieee.org/document/9028974

80. Controlled bidirectional converter using PID for charging battery in the stand-alone wind turbine system with Modified P&O to obtain MPPT (2017) IEEE Conference Publication | IEEE Xplore. https://ieeexplore.ieee.org/document/7925457

81. Agrawal A (2024) Circulating power flow restricted operation of the isolated bi-directional dual-active bridge DC-DC converter for battery charging applications. J Energy Storage 86:111123. https://doi.org/10.1016/j.est.2024.111123

82. Ashfaq MH, Jeyraj A, Selvaraj LP, Rahim N (2021) control strategies for bidirectional DC-DC converters: an overview. IOP Conf Ser Mater Sci Eng 1127(1):012031. https://doi.org/10.1088/1757-899x/1127/1/012031

83. Wang Y, Wu Y, Lee T (2013) Design and implementation of a bidirectional isolated dual-active-bridge-based DC/DC converter with dual-phase-shift control for electric vehicle battery. IEEE Energy Convers Congr Expos. https://doi.org/10.1109/ecce.2013.6647443

84. Sreelakshmi S, Deepa K (2015) Fuzzy based bidirectional converter. In: 2015 International conference on circuits, power and computing technologies [ICCPCT-2015]. https://doi.org/10.1109/iccpct.2015.7159398

85. Ezhil Reena Joy TP, Thirugnanam K, Kumar P (2012) A new concept for bidirectional inductively coupled battery charging system based on ac-dc-ac converter for PHEV's and EV's using fuzzy logic approach. In: 2012 IEEE transportation electrification conference and expo (ITEC), Dearborn, MI, USA, 2012, pp 1–6, https://doi.org/10.1109/ITEC.2012.6243432

86. Kumar S, Chauhan T, Rai S, Ali Z, Govindharaj A, Ambikapathy A (2021) Controlling bidirectional power flow of BESSs in DC microgrids using sliding mode controller. In: 2021 Asian conference on innovation in technology (ASIANCON), Pune, India, pp 1–7, https://doi.org/10.1109/ASIANCON51346.2021.9545024.

87. Bidirectional DC/DC converter based on the Model Predictive Control method: application to the Battery (2020) In: IEEE Conference Publication | IEEE Xplore. https://ieeexplore.ieee.org/document/9344025

88. Helal SA, Najee RJ, Hanna M, Shaaban MF, Osman A, Hassan MS (2017) An energy management system for hybrid microgrids in remote communities. In: Canadian conference on electrical and computer engineering (CCECE)-IEEE. https://doi.org/10.1109/ccece.2017.7946775

89. Sukumar S, Mokhlis H, Mekhilef S, Naidu K, Karimi M (2017) Mix-mode energy management strategy and battery sizing for economic operation of grid-tied microgrid. Energy 118:1322–1333. https://doi.org/10.1016/j.energy.2016.11.018

90. An LN, Tran QT (2015) Optimal energy management for grid connected microgrid by using dynamic programming method. IEEE Power Energy Soc General Meet. https://doi.org/10.1109/pesgm.2015.7286094

91. Strrelec M, Berka J (2013) Microgrid energy management based on approximate dynamic programming. IEEE PES ISGT Eur. https://doi.org/10.1109/isgteurope.2013.6695439

92. Choudar A, Boukhetala D, Barkat S, Brucker J (2015) A local energy management of a hybrid PV-storage based distributed generation for microgrids. Energy Convers Manag 90:21–33. https://doi.org/10.1016/j.enconman.2014.10.067

93. Sechilariu M, Wang B, Locment F (2013) Building-integrated microgrid: Advanced local energy management for forthcoming smart power grid communication. Energy Build 59:236–243. https://doi.org/10.1016/j.enbuild.2012.12.039

94. Chen C, Duan S, Cai T, Liu B, Hu G (2011) Smart energy management system for optimal microgrid economic operation. IET Renew Power Gener 5(3):258. https://doi.org/10.1049/iet-rpg.2010.0052

95. Radosavljević J, Jevtić M, Klimenta D (2015) Energy and operation management of a microgrid using particle swarm optimization. Eng Optim 48(5):811–830. https://doi.org/10.1080/0305215x.2015.1057135

96. Behera S, Choudhury, NBD (2023) Adaptive optimal energy management in multi-distributed energy resources by using improved slime mould algorithm with considering demand side management. e-Prime Adv Electr Eng Electron Energy 3:100108. https://doi.org/10.1016/j.prime.2023.100108

97. Behera S, Dev NB, Choudhury SB (2023) Maiden application of the Slime mold algorithm for optimal operation of energy management on a microgrid considering demand response Program. SN Comput Sci. https://doi.org/10.1007/s42979-023-02011-9

98. Alhasnawi BN, Jasim BH, Jasim AM, Bureš V, Alhasnawi AN, Homod RZ, Alsemawai MRM, Abbassi R, Sedhom BE (2023) A multi-objective improved cockroach swarm algorithm approach for apartment energy management systems. Information (Basel) 14(10):521. https://doi.org/10.3390/info14100521

99. Marzband M, Ghadimi M, Sumper A, Domínguez-García JL (2014) Experimental validation of a real-time energy management system using multi-period gravitational search algorithm for microgrids in islanded mode. Appl Energy 128:164–174. https://doi.org/10.1016/j.apenergy.2014.04.056

100. An IoT-Based smart microgrid system for rural areas (2022) IEEE Conference Publication | IEEE Xplore. https://ieeexplore.ieee.org/document/9976436

101. Chhaya L (2022) IoT-based management of smart microgrid: smart energy system. IGI Global eBooks, pp 833–842. https://doi.org/10.4018/978-1-6684-3666-0.ch036

102. Deowan ME, Nuhel AK, Sazid MM, Meghla RT, Haider I, Hazari MR (2023) Design and analysis of IoT-based adaptive microgrid system including renewable energy sources for decentralized zones. In: IEEE 2023 3rd international conference on robotics, electrical and signal processing techniques (ICREST). https://doi.org/10.1109/icrest57604.2023.10070093

103. Hafidz I, Priyadi A, Pujiantara M, Anggriawan DO, Purnomo MH (2023) Development of IoT-based portable power quality monitoring on microgrids by enhancing protection features. IEEE Access 11:49481–49492. https://doi.org/10.1109/access.2023.3276241

104. Alhasnawi BN, Jasim BH, Alhasnawi AN, Sedhom BE, Jasim AM, Khalili A, Bureš V, Burgio A, Siano P (2022) A novel approach to achieve MPPT for photovoltaic system based SCADA. Energies 15(22):8480. https://doi.org/10.3390/en15228480

105. Alhasnawi BN, Jasim BH, Mansoor R, Alhasnawi AN, Rahman ZSA, Alhelou HH, Guerrero JM, Dakhil AM, Siano P (2022) A

new Internet of Things based optimization scheme of residential demand side management system. IET Renew Power Gener 16(10):1992–2006. https://doi.org/10.1049/rpg2.12466

106. Alhasnawi BN, Jasim BH, Sedhom BE, Hossain E, Guerrero JM (2021) A new decentralized control strategy of microgrids in the internet of energy paradigm. Energies 14(8):2183. https://doi.org/10.3390/en14082183

107. Energy management system for small scale hybrid wind solar battery based microgrid (2020) IEEE Journals & Magazine | IEEE Xplore. https://ieeexplore.ieee.org/document/8950074

108. Iqbal MM, Kumar S, Lal C, Kumar C (2022) Energy management system for a small-scale microgrid. J Electr Syst Inf Technol. https://doi.org/10.1186/s43067-022-00046-1

109. Joshi S, Karamta M, Pandya B (2022) Small scale wind & solar photovoltaic energy conversion system for DC microgrid applications. Mater Today Proc 62:7092–7097. https://doi.org/10.1016/j.matpr.2022.01.461

110. Kumar PS (2021) Applications of hybrid wind solar battery based microgrid for Small-Scale Stand-Alone systems and grid integration for Multi-Feeder systems. Wiley Online Library, Amsterdam, pp 517–533

111. Roayaei M (2021) On the binarization of grey wolf optimizer: a novel binary optimizer algorithm. Research Square (Research Square). https://doi.org/10.21203/rs.3.rs-235817/v1

112. Al-Majidi SD, Abbod MF, Al-Raweshidy HS (2020) A particle swarm optimisation-trained feedforward neural network for predicting the maximum power point of a photovoltaic array. Eng Appl Artif Intell 92:103688. https://doi.org/10.1016/j.engappai.2020.103688

113. Sarma M, Sarma KK (2014) Fundamental considerations of ANN. Springer eBooks, New Delhi, pp 47–75

114. Arcos-Aviles D, Pascual JI, Guinjoan F, Marroyo L, Sanchís P, Marietta MP (2017) Low complexity energy management strategy for grid profile smoothing of a residential grid-connected microgrid using generation and demand forecasting. Appl Energy 205:69–84. https://doi.org/10.1016/j.apenergy.2017.07.123

115. Kuznetsova E, Li Y, Ruiz C, Zio E, Ault G, Bell K (2013) Reinforcement learning for microgrid energy management. Energy 59:133–146. https://doi.org/10.1016/j.energy.2013.05.060

116. Basantes JA, Castillo LDP, Llanos J, Ortiz D, Burgos-Mellado C (2023) Energy management system (EMS) based on model predictive control (MPC) for an isolated DC microgrid. Energies 16(6):2912. https://doi.org/10.3390/en16062912